Transportation Research Part B 84 (2016) 81–102

Contents lists available at ScienceDirect

Transportation Research Part B

journal homepage: www.elsevier.com/locate/trb

The impact of depot location, fleet composition and routing on emissions in city logistics

Çağrı Koç[a,b], Tolga Bektaş[b,*], Ola Jabali[c], Gilbert Laporte[a]

[a] CIRRELT, Canada Research Chair in Distribution Management and HEC Montréal, Montréal H3T 2A7, Canada
[b] Southampton Business School and Centre for Operational Research, Management Science and Information Systems (CORMSIS), University of Southampton, Southampton SO17 1BJ, United Kingdom
[c] CIRRELT and HEC Montréal, Montréal H3T 2A7, Canada

ARTICLE INFO

Article history:
Received 18 March 2015
Revised 15 December 2015
Accepted 16 December 2015

Keywords:
Location-routing
Fuel consumption
CO_2 emissions
Heterogeneous fleet
City logistics
Adaptive large neighborhood search metaheuristic

ABSTRACT

This paper investigates the combined impact of depot location, fleet composition and routing decisions on vehicle emissions in city logistics. We consider a city in which goods need to be delivered from a depot to customers located in nested zones characterized by different speed limits. The objective is to minimize the total depot, vehicle and routing cost, where the latter can be defined with respect to the cost of fuel consumption and CO_2 emissions. A new powerful adaptive large neighborhood search metaheuristic is developed and successfully applied to a large pool of new benchmark instances. Extensive analyses are performed to empirically assess the effect of various problem parameters, such as depot cost and location, customer distribution and heterogeneous vehicles on key performance indicators, including fuel consumption, emissions and operational costs. Several managerial insights are presented.

1. Introduction

City logistics poses challenges to governments, businesses, carriers, and citizens, particularly in the context of freight transportation, and calls for new business operating models. It also requires an understanding of the public sector and private businesses, as well as collaboration mechanisms to build innovative partnerships. Trade flows within cities exhibit a high variability, both in the size and shape of the shipments. Cities often possess a transportation infrastructure that allows traffic flows within their boundaries, but this infrastructure is often inadequate for freight transportation, which translates into congestion and pollution. For relevant references and more detailed information on city logistics, the reader is referred to the books of Taniguchi et al. (2001) and of Gonzalez-Feliu et al. (2014).

Depot location, fleet composition and routing all bear on emissions in urban freight transportation. Some of their interactions are already well documented. However, whereas there exists an extensive body of knowledge on the integration of location and routing, on the effect of route choice on pollution and on the impact of fleet composition on emissions, the interplay between depot location, fleet composition and routing decisions and their influence on emissions has not yet been investigated. Yet, these decisions are clearly intertwined, especially in a city logistics context. Our purpose is to analyze these three interrelated components of city logistics within a unified framework. Before we proceed with our study, we briefly review the relevant literature on some of the interactions just mentioned.

* Corresponding author. Tel.: +44 2380598969.
E-mail addresses: Cagri.Koc@cirrelt.ca (Ç. Koç), T.Bektas@soton.ac.uk (T. Bektaş), Ola.Jabali@hec.ca (O. Jabali), Gilbert.Laporte@cirrelt.ca (G. Laporte).

http://dx.doi.org/10.1016/j.trb.2015.12.010
0191-2615/

1.1. A brief review of the literature

Depot location and vehicle routing are two interdependent decisions. Their joint study was first suggested by Von Boventer (1961) and has since evolved into what is now commonly known as the Location-Routing Problem (LRP) (see Laporte et al., 1988; Min et al., 1998; Nagy and Salhi, 2007; Prodhon and Prins, 2014; Albareda-Sambola et al., 2015; Drexl and Schneider, 2015, for reviews). Applications of the LRP arise namely in city logistics (Boudoin et al., 2014; Mancini et al., 2014).

Fleet composition is yet another critical issue in city logistics. Heterogeneous vehicle fleets are commonly used in most distribution problems (Hoff et al., 2010). Heterogeneous VRPs include two major classes: the Fleet Size and Mix Vehicle Routing Problem proposed by Golden et al. (1984), which works with an unlimited fleet, and the Heterogeneous Vehicle Routing Problem (HVRP) introduced by Taillard (1999), which works with a known fleet. For further details on these problems and their variants, we refer the reader to Baldacci et al. (2008), Jabali et al. (2012a) and Koç et al. (2016b). In recent years, green issues have received increased attention in the context of the HVRP (see Kopfer et al., 2013, 2014; Kwon et al., 2013). Koç et al. (2014) introduced the Fleet Size and Mix Pollution-Routing Problem which extends the Pollution-Routing Problem (PRP) by considering a heterogeneous vehicle fleet and developed a hybrid evolutionary metaheuristic to solve it. They conducted computational experiments to shed light on the trade-offs between various performance indicators, such as fuel and CO_2 emissions, vehicle fixed cost, distance, driver cost and total cost. They demonstrated the benefit of using a heterogeneous fleet over a homogeneous one.

Greenhouse gases (GHGs) are a noxious by-product of road freight transportation (Kirby et al., 2000) which accounts for around a quarter of the total GHG emissions in the United Kingdom and the United States (DfT, 2012; EPA, 2012). The relationship between road freight transportation and emissions has been the object of several studies in recent years. Thus Demir et al. (2011) have surveyed several estimation models for fuel consumption and greenhouse gas emissions. More specifically, the authors have compared six models and have assessed their respective strengths and weaknesses. These models indicate that fuel consumption depends on a number of factors that can be grouped into four categories: vehicle, driver, environment and traffic. Figliozzi (2011) simultaneously considered the effects of GHG costs, new engine technologies, market conditions and fiscal policies in fleet management models. The author proposed an integer programming vehicle replacement model in order to compute some environmental and political indicators. Four factors were analyzed in scenarios arising from a case study in Portland, Oregon, namely annual vehicle utilization, gasoline prices, electric vehicle tax credits, and GHG emissions costs. Bigazzi and Figliozzi (2012) examined several factors affecting GHGs emissions. The authors focused on the effects of travel demand flexibility and on the characteristics of two types of vehicles, namely light and heavy duty, across different types of pollutants. They stated that fleet composition and vehicle type are key factors driving CO_2 emissions. Furthermore, the authors indicated that several demand- or vehicle-based emissions strategies could have an impact on the reduction of CO_2 emissions. Jabali et al. (2012b) later studied the trade-off between the minimization of CO_2 emissions and that of total travel times in the context of the time-dependent Vehicle Routing Problem (VRP) in which the planning horizon is partitioned into two phases: free flow traffic and congestion. The authors solved the problem using tabu search and proposed efficient bounding procedures. More recently, Ehmke et al. (2014) studied stochastic shortest paths with an emissions minimization objective. The authors concluded that in order to minimize emissions, vehicles may have to travel via a circuitous path rather than along a more direct shortest path.

The Pollution-Routing Problem (PRP), introduced by Bektaş and Laporte (2011), is an extension of the classical VRP with time windows. It consists of routing vehicles to serve a set of customers, and of determining their speed on each route segment to minimize a function comprising fuel cost, emissions and driver costs. To estimate fuel consumption, the authors applied a simplified version of the emission and fuel consumption model proposed by Barth et al. (2005), Scora and Barth (2006) and Barth and Boriboonsomsin (2009). This simplified model assumes that all parameters will remain constant on a given arc, but load and speed may change from one arc to another. As such, the PRP objective approximates the total amount of energy consumed on a given road segment, which directly translates into fuel consumption and further into GHG emissions. Demir et al. (2012) developed an extended adaptive large neighborhood search (ALNS) heuristic for the PRP. This heuristic operates in two stages: the first stage is an extension of the classical ALNS scheme to construct vehicle routes (Pisinger and Ropke, 2007; Ropke and Pisinger, 2006a, 2006b), and the second stage applies a speed optimization algorithm (SOA) (Hvattum et al., 2013; Norstad et al., 2010) to compute the speed on each arc. In a later study, Demir et al. (2014a) introduced the bi-objective PRP which jointly minimizes fuel consumption and driving time. The authors have developed a bi-objective adaptation of their ALNS-SOA heuristic and compared four *a posteriori* methods, namely the weighting method, the weighting method with normalization, the epsilon-constraint method and a new hybrid method, using a scalarization of the two objective functions. Franceschetti et al. (2013) studied the time-dependent PRP under a two-stage planning horizon, as in Jabali et al. (2012b), and developed an explicit congestion model in addition to the PRP objectives. The authors presented a mathematical formulation in which vehicle speeds are optimally selected from a set of discrete values. More recently, Kramer et al. (2015) proposed a matheuristic for the PRP, as well as for the Fuel Consumption VRP and the Energy Minimizing VRP, which integrates iterated local search with a set partitioning procedure and an SOA. Their method outperformed those presented in previous studies and yielded new best-known solutions. Zhang et al. (2015) proposed an evolutionary local search heuristic for the minimization of fuel consumption under three dimensional loading constraints. Fatnassi et al. (2015) investigated energy gains arising from joint goods and passenger transportation. For a

Table 1
Parameters common to all vehicle types.

Notation	Description	Typical values
ξ	Fuel-to-air mass ratio	1
g	Gravitational constant (m/s^2)	9.81
ρ	Air density (kg/m^3)	1.2041
C_r	Coefficient of rolling resistance	0.01
η	Efficiency parameter for diesel engines	0.45
f_c	Fuel and CO_2 emissions cost (£/L)	1.4
κ	Heating value of a typical diesel fuel (kJ/g)	44
ψ	Conversion factor (g/s to L/s)	737
n_{tf}	Vehicle drive train efficiency	0.45
θ	Road angle	0
τ	Acceleration (m/s^2)	0

Table 2
Vehicle-specific parameters.

Notation	Description	Light duty 1 (L1)	Light duty 2 (L2)	Medium duty (M)
w^h	Curb weight (kg)	3500	4500	5500
Q^h	Maximum payload (kg)	4000	7500	12,500
μ^h	Vehicle fixed cost (£/day)	42	49	60
k^h	Engine friction factor (kJ/rev/L)	0.25	0.23	0.20
N^h	Engine speed (rev/s)	38.34	37.45	36.67
V^h	Engine displacement (L)	4.5	4.5	6.9
C_d^h	Coefficient of aerodynamics drag	0.6	0.64	0.7
A^h	Frontal surface area (m^2)	7.0	7.4	8.0

state-of-the-art coverage on green road freight transportation, the reader is referred to the book chapter of Eglese and Bektaş (2014), and to the surveys of Demir et al. (2014b) and Lin et al. (2014).

1.2. Scientific contributions and structure of the paper

This paper studies the joint impact of location, fleet composition and routing on emissions in a city logistics context. It makes three main scientific contributions. Its first contribution is to formally model this new problem and solve it by means of a powerful ALNS metaheuristic. Its second contribution is to carry out extensive computational experiments and analyses in order to gain a deep understanding into the interactions between the components of the problem. Its third contribution is to provide managerial insights.

The remainder of this paper is structured as follows. Section 2 presents a general framework for our analysis. Section 3 provides a formal description of the problem and a mathematical formulation. Section 4 contains a brief description of the proposed metaheuristic. Extensive computational experiments, including a validation of our algorithm and sensitivity analyses, are presented in Section 5, followed by conclusions and managerial insights in Section 6.

2. General description of the problem setting

We will first briefly provide our fuel consumption and CO_2 emissions model in Section 2.1. We will then describe the vehicle types and their characteristics in Section 2.2, followed by the specification of speed zones in Section 2.3, by the network structure in Section 2.4, and by the depot costs in Section 2.5.

2.1. Fuel consumption and CO_2 emissions

We use the comprehensive emissions model of Barth et al. (2005), Scora and Barth (2006), and Barth and Boriboonsomsin (2008) to estimate fuel consumption and emissions at a given time instant. This model has already been successfully applied to the PRP (Bektaş and Laporte, 2011; Demir et al., 2012) and to some of its extensions (Demir et al., 2014a; Franceschetti et al., 2013; Koç et al., 2014). In what follows, we briefly recall the heterogeneous fleet version of this model (Koç et al., 2014), where the index set of vehicle types is denoted by $\mathcal{H}$. The fuel consumption rate FR^h (L/s) of a vehicle of type $h \in \mathcal{H}$ is given by

$$FR^h = \xi (k^h N^h V^h + P^h/\eta)/\kappa, \tag{1}$$

where the variable P^h is the second-by-second engine power output (in kW) of vehicle type h, and other parameters that appear in the equation are given in Tables 1 and 2. Variable P^h can be calculated as

$$P^h = P^h_{tract}/n_{tf} + P_{acc}, \tag{2}$$

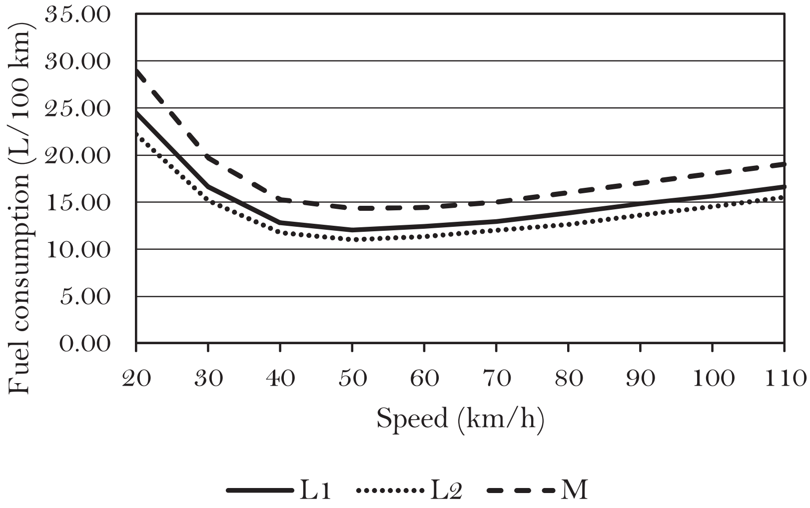

Fig. 1. Fuel consumption as a function of speed.

where the engine power demand P_{acc} is associated with the running losses of the engine and the operation of vehicle accessories such as air conditioning and electrical loads. We assume that $P_{acc} = 0$. The total tractive power requirement P^h_{tract} (in kW) for a vehicle of type h is

$$P^h_{tract} = (M^h\tau + M^h g \sin\theta + 0.5C^h_d \rho A v^2 + M^h g C_r \cos\theta)v/1000, \tag{3}$$

where M^h is the total vehicle weight (in kg) and v is the instantaneous vehicle speed (m/s). The fuel consumption F^h (L) of vehicle type h over a distance d traveling at constant speed v is calculated as

$$F^h = k^h N^h V^h \lambda d/v \tag{4}$$

$$+ P^h \lambda \gamma d/v, \tag{5}$$

where $\lambda = \xi/\kappa\psi$ and $\gamma = 1/1000 n_{tf}\eta$ are constants. Let $\beta^h = 0.5C^h_d \rho A^h$ be a vehicle-specific constant and $\alpha = \tau + g\sin\theta + gC_r\cos\theta$ be a vehicle-arc specific constant. Therefore, F^h can be rewritten as

$$F^h = \lambda(k^h N^h V^h d/v + M^h \gamma\alpha d + \beta^h \gamma d v^2). \tag{6}$$

In this expression the first term $k^h N^h V^h d/v$ is called the engine module, which is linear in travel time. The second term $M^h\gamma\alpha d$ is referred to as the weight module, and the third term $\beta^h\gamma d v^2$ is the speed module, which is quadratic in speed. These functions will be used in the objective function of the mathematical formulation in Section 3.

2.2. Vehicle types and characteristics

We consider three vehicle types produced by MAN (2015a), a major truck manufacturer whose market share in Western Europe was around 16.3% in 2013 (Statista, 2013). These three vehicle types include two light duty (TGL) vehicles and one medium duty (TGM) vehicle, classified as single-unit trucks by FHWA (2011). Table 1 lists the values of the parameters (Demir et al., 2012, 2014a; Franceschetti et al., 2013; Koç et al., 2014) common to all vehicle types, while Table 2 lists specific parameters (MAN, 2015a, 2015b, 2015c) for each vehicle type. We refer the reader to MAN (2015a, 2015b, 2015c) for further details on TGL and TGM vehicles and their engines.

The fuel consumption function (6) per unit distance traveled as a function of speed is typically U-shaped (Fig. 1) and results in an optimal speed that minimizes the fuel consumption. This function is the sum of two components, one induced by (4) and the other by (5), and is plotted for the three vehicle types considered in this paper.

2.3. Arc-specific speeds and speed zones

Road speed limits are commonly set by national or local governments (Wikipedia, 2015). They play a key role in ensuring the safety of road users and of the public at large (UK Government, 2014). While most cities impose arc-specific speed limits, some are often divided into speed zones (e.g., Dublin City Council, 2015), which can be viewed as a special case of arc-speed limits. Speed zones help traffic flow more safely and efficiently. They provide a reasonable balance between the needs of drivers, pedestrians and cyclists who use public roads for travel, and the concerns of residents who live along these roads (Oregon, 2015). Studies have been performed in the United Kingdom by the Department for Transport (DfT, 2013), in Canada by the City of Ottawa Transportation Committee (2009) and in the United States by the

Fig. 2. Grid city examples (Google Maps, 2015).

Oregon Department of Transportation (2015) on the best way to establish speed zones. These studies indicate that setting reasonable vehicle speeds for a variety of weather conditions results in fewer accidents. When reasonable speeds are imposed, less overtaking occurs, and one also observes smaller delays and fewer rear-end collisions. According to the above studies, speed zones in cities are generally classified under three categories:

- 15 mph (25 km/h): alleys, narrow residential roadways,
- 20 mph (32 km/h): business districts, school zones,
- 25 mph (40 km/h): residential districts, public parks, ocean shores.

Speed zones also yield environmental benefits. For example Kirkby (2002) states that 20 mph (32 km/h) speed zones, significantly improve the quality of life of the concerned community, and encourage healthier and more sustainable transportation. This speed limit favors slower driving, saves fuel and reduces pollution, unless an unnecessarily low gear is used (DfT, 2013). Van Woensel et al. (2001) noted that vehicles must often travel at traffic speed in urban areas, and changes in speed have a significant impact on CO_2 emissions. The model we introduce in Section 3 works with a constant speed throughout the day, which does not capture potential speed variations due traffic congestion that may occur over time. A natural extension to this paper would be to add a temporal dimension to the problem enabling the incorporation of time-dependent speeds to account for traffic congestion.

2.4. Network structure

We consider cities represented by a finite graph $\bar{G} = (\bar{N}, \bar{A})$ in which distances are measured using the Taxicab geometry (see Krause, 2012). The Taxicab geometry is also known as the rectilinear distance, the L_1 distance, the city block distance or the Manhattan distance. It implies that the shortest path between two nodes is the sum of horizontal and vertical distances between them. This metric is appropriate in several grid cities, such as Glasgow, Ottawa and Portland, shown in Fig. 2.

In the primary setting considered in this study (see Section 5.7 for an exception), we assume that the city center is divided into several zones, each belonging to one of the three categories described in Section 2.3. For example, if there are three zones then, zone 1 would correspond to the city center, zone 2 would be an outer urban area, and zone 3 would be a suburb. In this case, let V_1, V_2, V_3 be the fixed speeds in zones 1, 2, 3, respectively, where $V_1 < V_2 < V_3$. Fig. 3 illustrates a city divided into three such speed zones. We assume that the depots and the customers are located on a grid superimposed on the zones and that the zone boundaries coincide with segments of the horizontal or vertical lines of the grid. As a result, any segment linking two consecutive points of the grid will lie entirely within the same speed zone. The granularity of the grid can be arbitrarily fine. When a vehicle travels within the same zone, its speed is equal to the speed of that zone. When it travels on the boundary of two speed zones, it uses the faster speed of the two zones.

In a city, a shortest path between i and j is not necessarily a cheapest or a least polluting path. In urban areas where a maximum speed limit of 40 km/h is imposed, a fastest path is also a least-polluting path according to Fig. 1. However, as in Ehmke et al. (2014), this path is not always a shortest path. For example, consider the corners (A, B, C, D) of zone 2 in Fig. 3, and nodes i and j located in zone 3. When traveling from i to j, a vehicle may not travel on a straight line from i to j with speed V_2 between points K and L, but may instead travel on the boundaries of zone 2 with speed $V_3 \le 40$ km/h to avoid driving at a slower speed through congested traffic. A fastest path from customer i to j could well be (i, K, A, C, L, j) instead of (i, K, L, j), particularly in urban settings.

Using $F^h = \lambda(k^h N^h V^h d/v + M^h \gamma \alpha d + \beta^h \gamma d v^2)$, we now illustrate how the load on a vehicle can affect the calculation of the cheapest path between a node pair. In Fig. 3, assume that the total length of path is 8 km for (i, K, L, j), and 9 km for (i, K, A, C, L, j). More specifically it is 0.5 km for (i, K), (K, A), (L, J) and (L, C), and 7 km for (K, L) and (A, C). When a medium duty vehicle going from i to j carries a load equal to 1000 kg, then the cost of (i, K, L, j) is £1.85 and the cost of (i, K, A, C,

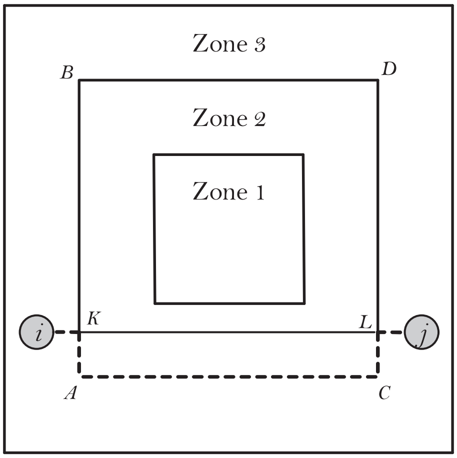

Fig. 3. Illustration of speed zones.

L, j) is £1.95 with the former path being the cheaper one. However, when the vehicle load is equal to 12,500 kg, then the cost of (i, K, L, j) is £2.20 and the cost of (i, K, A, C, L, j) is £2.05, where the cheapest path now is the latter.

2.5. Depot costs

There are four main categories of depot or warehouse costs: handling, storage, operations administration and general administrative expenses (see Ghiani et al., 2013). Storage expenses are the cost of occupying a facility (Speh, 2009). Depot location affects the storage cost, e.g., locating a depot in the city center (zone 1) is much more expensive than locating it in an outer zone (zone 2 or 3).

3. Formal problem description and mathematical formulation

Our problem is defined on a complete directed graph $\mathcal{G} = (\mathcal{N}, \mathcal{A})$, where $\mathcal{N} = (\mathcal{N}_0 \cup \mathcal{N}_c) \subseteq \bar{N}$ is a set of nodes in which $\mathcal{N}_0$ and $\mathcal{N}_c$ represent the potential depots and customer nodes, respectively. A storage capacity D_k and a fixed opening cost g_k are associated with each potential depot $k \in \mathcal{N}_0$. Each customer $i \in \mathcal{N}_c$ has a positive demand q_i. The arc set $\mathcal{A}$ is defined as $\mathcal{A} = \{(i,j) : i \in \mathcal{N}, j \in \mathcal{N}, i \neq j\} \setminus \{(i,j) : i \in \mathcal{N}_0, j \in \mathcal{N}_0, i \neq j\}$. We assume that an unlimited heterogeneous fleet of vehicles operates with various capacities and vehicle-related costs. The index set of vehicle types is denoted by $\mathcal{H}$. Let Q^h and t^h denote the capacity and fixed dispatch cost of a vehicle of type $h \in \mathcal{H}$, respectively. Let f_{ij}^h be the amount of commodity carried by a vehicle of type h from node i to node j. We denote by $c(i, j, f_{ij}^h)$ fuel and CO_2 emissions cost of traveling from node i to node j with a vehicle of type h having a load equal to f_{ij}^h upon leaving i. This cost is calculated using equation (6). Since an arc (i, j) in graph $\mathcal{G}$ corresponds to one or more consecutive segments on the grid, the calculation of the cost function $c(i, j, f_{ij}^h)$ will take into account the different speeds associated with these segments. If node $i \in \mathcal{N}_0$, then f_{ij}^h is equal to the total load of the route of a vehicle of type h assigned to depot i.

The problem consists of locating depots in a subset of $\mathcal{N}_0$, assigning each customer to a depot, determining a set of vehicle routes such that all vehicles start and end their routes at their depot, such that the load of each vehicle does not exceed its capacity. The objective is to minimize the total cost which is made up of three components: the depot operating cost, the vehicle fixed cost, and the fuel and CO_2 emissions cost. Furthermore, the speed of a vehicle depends on the speeds of the arcs it traverses while driving.

To formulate the problem, we define the following additional decision variables. Let x_{ij}^h be equal to 1 if a vehicle of type $h \in \mathcal{H}$ travels on arc $(i, j) \in A$ and to 0 otherwise. Let u_k be equal to 1 if depot $k \in \mathcal{N}_0$ is opened and to 0 otherwise. Let z_{ik} be equal to 1 if customer $i \in \mathcal{N}_c$ is assigned to depot $k \in \mathcal{N}_0$ and to 0 otherwise.

A mathematical formulation of the problem is given as follows:

$$\text{Minimize} \sum_{k \in \mathcal{N}_0} g_k u_k + \sum_{h \in \mathcal{H}} \sum_{k \in \mathcal{N}_0} \sum_{j \in \mathcal{N}_c} t^h x_{kj}^h + \sum_{h \in \mathcal{H}} \sum_{(i,j) \in \mathcal{A}} c(i, j, f_{ij}^h) x_{ij}^h \tag{7}$$

subject to

$$\sum_{h \in \mathcal{H}} \sum_{j \in \mathcal{N}} x_{ij}^h = 1 \quad i \in \mathcal{N}_c \tag{8}$$

$$\sum_{h\in\mathcal{H}}\sum_{j\in\mathcal{N}} x_{ji}^h = \sum_{h\in\mathcal{H}}\sum_{j\in\mathcal{N}} x_{ij}^h \quad i\in\mathcal{N} \tag{9}$$

$$\sum_{h\in\mathcal{H}}\sum_{j\in\mathcal{N}} f_{ji}^h - \sum_{h\in\mathcal{H}}\sum_{j\in\mathcal{N}} f_{ij}^h = q_i \quad i\in\mathcal{N}_c \tag{10}$$

$$f_{ij}^h \le Q^h x_{ij}^h \quad i\in\mathcal{N}_0, j\in\mathcal{N}, i\neq j, h\in\mathcal{H} \tag{11}$$

$$\sum_{h\in\mathcal{H}}\sum_{j\in\mathcal{N}_c} f_{kj}^h = \sum_{j\in\mathcal{N}_c} z_{jk} q_j \quad k\in\mathcal{N}_0 \tag{12}$$

$$\sum_{h\in\mathcal{H}}\sum_{j\in\mathcal{N}_c} f_{jk}^h = 0 \quad k\in\mathcal{N}_0 \tag{13}$$

$$f_{ij}^h \le (Q^h - q_i) x_{ij}^h \quad i\in\mathcal{N}_c, j\in\mathcal{N}, h\in\mathcal{H} \tag{14}$$

$$f_{ij}^h \ge q_j x_{ij}^h \quad i\in\mathcal{N}, j\in\mathcal{N}_c, h\in\mathcal{H} \tag{15}$$

$$\sum_{i\in\mathcal{N}_c} q_i z_{ik} \le D_k u_k \quad k\in\mathcal{N}_0 \tag{16}$$

$$\sum_{k\in\mathcal{N}_0} z_{ik} = 1 \quad i\in\mathcal{N}_c \tag{17}$$

$$x_{ij}^h + \sum_{q\in\mathcal{H}, q\neq h}\ \sum_{r\in\mathcal{N}, j\neq r} x_{jr}^q \le 1 \quad i\in\mathcal{N}, j\in\mathcal{N}_c, i\neq j, h\in\mathcal{H} \tag{18}$$

$$\sum_{h\in\mathcal{H}} x_{ik}^h \le z_{ik} \quad k\in\mathcal{N}_0, i\in\mathcal{N}_c \tag{19}$$

$$\sum_{h\in\mathcal{H}} x_{ki}^h \le z_{ik} \quad k\in\mathcal{N}_0, i\in\mathcal{N}_c \tag{20}$$

$$\sum_{h\in\mathcal{H}} x_{ij}^h + z_{ik} + \sum_{m\in\mathcal{N}_0, m\neq k} z_{jm} \le 2 \quad k\in\mathcal{N}_0, (i,j)\in\mathcal{N}_c, i\neq j \tag{21}$$

$$x_{ij}^h \in \{0,1\} \quad i,j\in\mathcal{N}, h\in\mathcal{H} \tag{22}$$

$$u_k \in \{0,1\} \quad k\in\mathcal{N}_0 \tag{23}$$

$$z_{ik} \in \{0,1\} \quad k\in\mathcal{N}_0, i\in\mathcal{N}_c \tag{24}$$

$$f_{ij}^h \ge 0 \quad (i,j)\in\mathcal{N}, h\in\mathcal{H}. \tag{25}$$

The objective function (7) minimizes the total cost including fixed depot and vehicle costs, as well as fuel and CO_2 emissions cost. Constraints (8) and (9) ensure that each customer is visited exactly once. Constraints (10) imply that the demand of each customer is fully served. Constraints (11) mean that the total load on any path cannot exceed the capacity of the vehicle traversing it. Constraints (12) ensure that the total load of the vehicles departing from a depot is equal to the total demand of the customers assigned to it. Constraints (13) state that the load on all vehicles returning to each depot must be equal to zero. Constraints (14) and (15) are the bounds on the load variables. Constraints (16) guarantee that total demand associated with a depot cannot exceed its capacity. Constraints (17) and (18) ensure that each customer is assigned to only one depot and one vehicle, respectively. Constraints (19)–(21) forbid the formation of routes that do not start and end at the same depot. Finally, constraints (22)–(25) enforce the integrality and non-negativity restrictions on the variables.

4. Description of the ALNS metaheuristic

The mathematical formulation just presented is of large scale and cannot be solved for most practical instances. We have therefore devised a metaheuristic algorithm, called pollution-and-location-heterogeneous adaptive large neighborhood search (P-L-HALNS), to solve the problem. This algorithm is partly based on the ALNS framework of Demir et al. (2012) which was initially put forward by Ropke and Pisinger (2006a, 2006b) to solve several variants of the VRP (see Laporte et al., 2014). This metaheuristic has since provided very good results on several complicated variants of the VRP (see Pisinger and Ropke, 2007; Koç et al., 2015a), of the LRP (see Koç et al., 2016a), and of the PRP (see Demir et al., 2012, 2014a; Koç et al., 2014).

The P-L-HALNS consists of two basic procedures: removal or destroy, followed by insertion or repair. In the removal procedure, n' nodes are iteratively removed by destroy operators and placed in the removal list, where n' lies in the interval $[b_l, b_u]$ for the destroy operators. In the insertion procedure, the nodes of the removal list are iteratively inserted into a least-cost position of the incomplete solution by means of an insertion operator. The removal and insertion operators are selected dynamically according to their past performance. To this end, each operator is assigned a score which is increased whenever it improves the current solution and is periodically reset to one. Simulated annealing is used as an outer local search framework for the P-L-HALNS in order to define the acceptance rule of candidate solutions.

In order to perform least-cost insertions, it is necessary to frequently make use of cheapest path values during the course of the algorithm. We explain in Section 4.1 how these computations are handled in the ALNS metaheuristic. This is followed in Section 4.2 by an overview of the metaheuristic itself.

4.1. Cheapest path calculation for speed zones

The number of undominated paths between any two nodes in $\bar{G}$ is finite, but the identification of such paths is not trivial since the cost of a path depends on the type of vehicle traveling a path from i to j, on its load upon leaving i, and on the speed of each arc of the path (see Eq. (6)). To overcome the complexity of this task, we introduce the Cheapest Path Calculation heuristic which simplifies computations in speed zone settings. This heuristic computes z paths between i and j for z speed zones and selects the cheapest one. This procedure does not guarantee the calculation of the minimum cost path over all possible paths, but is suitable for iterative use within an algorithm like the P-L-HALNS described here.

Algorithm 1 Cheapest path calculation.

```
1: Consider nodes i ∈ N and j ∈ N \ {i}. ν ← 0.
2: Apply Two Paths (i, j)
3: ν ← ν + 1
4: while ν < z do
5:     Apply Alternative Paths (i, j, p_0)
6:     ν ← ν + 1
7: end while
8: Return Least cost path p_k where k = arg min {χ_0, χ_1, ..., χ_{z−1}}
```

Algorithm 1 presents this procedure for a node pair (i, j) and for finite z speed zones. We first find a path between i and j by Algorithm 2 (lines 2–4). According to the Taxicab geometry (see Section 2.4), if node i and j are not located on the same horizontal nor on the same vertical coordinate, there exist several shortest paths with the same length, but not necessarily with the same cost for a vehicle with a fixed load, because of the possibility for the vehicle to travel through several zones. In Algorithm 2, we form two paths, one that first traverses the X coordinate, and then the Y coordinate. The rule for the other path is the opposite, first Y, then X. We identify the cheapest path p_0 of the two and discard the other one. We then iteratively contort p_0 to generate alternative paths $p_1, \ldots, p_{z-1}$ (lines 5–9) in Algorithm 3, in which we compare the costs of $p_0, p_1, \ldots, p_{z-1}$, and take the cheapest path (line 10). In this algorithm, a path p_ν follows the boundary of zone ν on which it travels at a speed $V_{\nu+1}$ based on the assumption made in Section 2.4. We do not consider travel on or outside the boundary of zone z since this is not defined. It should be noted that in the P-L-HALNS, we calculate the cheapest path between each pair of nodes a priori, as is commonly done in the VRP.

Fig. 4 illustrates the Cheapest Path Calculation procedure for a given node pair (i, j), the three speed zones considered in this paper and a vehicle with a fixed load traveling between these nodes. Fig. 4a shows the formation of two paths by the Two Paths algorithm, (i, A, j) and (i, B, j) that are the shortest with respect to the Taxicab geometry, but the cheapest path would always be (i, B, j) since $V_2 < V_3 \leq 40$ km/h. We then calculate the cost χ_0 of $p_0 = (i, B, j)$. Fig. 4b and c shows the formation of the two paths described in Algorithm 3. In Fig. 4b, we first find the shortest path from node i to nearest point A_ν of zone 1. We then find the shortest path, on the border of zone 1, from point A_ν to nearest point B_ν of zone 1 to node j. We finally find the shortest path from point B_ν to node j. As in Step 1, if there are two same length shortest paths between points, such as (B_ν, B_ν^1, j) and (B_ν, B_ν^2, j), we select the cheapest one, in this case (B_ν, B_ν^1, j). We calculate the cost χ_1 of $p_1 = (i, A_\nu, B_\nu, B_\nu^1, j)$. In Fig. 4c, we first find the shortest path from node i to nearest point A_ν of zone 2. We then find the shortest path, on the border of zone 2, from point A_ν to nearest point B_ν of zone 2 to node j. We finally find the shortest path from point B_2 to node j. We calculate the cost χ_2 of $p_2 = (i, A_\nu, B_\nu, j)$.

Algorithm 2 Two paths.

Input: i, j
if i and j are located neither on the same horizontal nor the same vertical coordinate **then**
    Find two paths 1 (p_0^1) and 2 (p_0^2) between i and j. p_0^1 that first traverses the X coordinate, and then the Y coordinate. The rule for the p_0^2 is the opposite, first Y, then X.
    Calculate costs χ_0^1 and χ_0^2 of paths p_0^1 and p_0^2
    if $\chi_0^1 \leq \chi_0^2$ **then**
        $p_0 \leftarrow p_0^1$
        $\chi_0 \leftarrow \chi_0^1$
    else
        $p_0 \leftarrow p_0^2$
        $\chi_0 \leftarrow \chi_0^2$
else
    Find shortest path p_0 between (i, j)
    Calculate the cost χ_0 of path p_0
Return p_0 and χ_0

It is relatively easy to find cases for which this procedure does not identify an optimal path. However, the precise calculation of departure from optimality requires further research.

4.2. Overview of the metaheuristic

The general framework of the P-L-HALNS metaheuristic is sketched in Algorithm 4. We now briefly explain its steps. Given the complexity of implementing the Cheapest Path Calculation procedure at every step of the P-L-HALNS, we work with average route demand lengths. At the beginning of the algorithm, we first define a set $\mathcal{B}$ of average route demand levels. The total demand of customers is known a priori. For example, let $|\mathcal{B}| = 4$ and the total demand be 2000 kg, which results in the following intervals: level 1 ranges from 0 to 500 kg, level 2 ranges from 501 to 1000 kg, level 3 ranges from 1001 to 1500 kg, and level 4 ranges from 1501 to 2000 kg. Let $\upsilon_{ij}^{\beta h}$ be the fixed cost associated with the path for each average route demand level $\beta \in \mathcal{B}$ and for each vehicle of type $h \in \mathcal{H}$. The fixed costs $\upsilon_{ij}^{\beta h}$ are calculated at the beginning of the algorithm (line 1). These fixed costs are used to compute the route costs quickly. During the algorithm, for each solution, the average route demand is calculated as (total demand of customers)/(total number of vehicle routes). In the above example, if the number of vehicle routes is three, then the average route demand is 2000/3 which is at level $\beta = 2$ ($\beta \in \mathcal{B}$).

An initial solution ω_0 is generated by using a modified version of the classical Clarke and Wright (1964) savings algorithm for the VRP (line 2). The selection probabilities are initialized for each destroy and repair operator (line 3). In line 4, ω_b is the best solution found during the search, ω_c is the current solution obtained at the beginning of an iteration, and ω_t is a temporary solution found at the end of the iteration which can be discarded or become the current solution. The temperature is denoted by T, the iteration counter is denoted by j, and the current and the best solutions are initially set equal to the initial solution (line 4). The temperature T is initially set at $c(\omega_0)P_0$, where $c(\omega_0)$ is the cost of initial solution and P_0 is the initial temperature.

Every σ iterations, a diversification based removal operator is selected (lines 6–8) and applied to ω_c; otherwise an intensification based removal operator is selected (lines 9–11). An insertion operator is then selected and applied to the destroyed solution, and a feasible solution ω_t is obtained (line 12).

The operators are iteratively applied using the average costs up until the counter p reaches ς, following which the actual costs for ω_c, ω_t and ω_b are calculated using the Cheapest Path Calculation procedure (Algorithm 1), and the counter p is reset to zero (lines 13–15); otherwise, the fixed costs are used to compute $c(\omega_t)$ (lines 16–18). If the cost of a repaired solution $c(\omega_t)$ is less than that of the current solution $c(\omega_c)$, then ω_c is replaced by ω_t (lines 19 and 20); otherwise, the probability ϑ of accepting a non-improving solution is computed (lines 21 and 22) as a function of the current temperature and of the value of $c(\omega_t) - c(\omega_c)$. A random number ϵ is then generated in the interval [0, 1] (line 23). If ϵ is less than ϑ, ω_c is then replaced by ω_t (lines 24 and 25). If the cost of ω_c is less than that of ω_b, ω_b is replaced by ω_c (lines 26 and 27). The current temperature is gradually decreased during the algorithm as δT (line 28), where $0 < \delta < 1$ is a fixed cooling parameter. The probabilities are updated by means of an adaptive weight adjustment procedure (AWAP) every ζ iteration (line 29). When the maximal number ϖ iterations is reached, the algorithm terminates (line 31) and returns the best found solution. For further information on the operators and on other algorithmic details the reader is referred to Demir et al. (2012) and Koç et al. (2016a).

Algorithm 3 Alternative paths.

Input: i, j and p_0
Step 1
Find the shortest path from node i to nearest point (A_ν) on an edge of zone ν
if there are several same length shortest paths between i and A_ν **then**
    Select two paths: $p(i, A_\nu^1, A_\nu)$ and $p(i, A_\nu^2, A_\nu)$ where A_ν^1 and A_ν^2 are the intersection points of X and Y coordinates
    Calculate costs $\chi(i, A_\nu^1, A_\nu)$ and $\chi(i, A_\nu^2, A_\nu)$ of paths $p(i, A_\nu^1, A_\nu)$ and $p(i, A_\nu^2, A_\nu)$
    if $\chi(i, A_\nu^1, A_\nu) \leq \chi(i, A_\nu^2, A_\nu)$ **then**
        $p(i, A_\nu) \leftarrow p(i, A_\nu^1, A_\nu)$
        $\chi(i, A_\nu) \leftarrow \chi(i, A_\nu^1, A_\nu)$
    else
        $p(i, A_\nu) \leftarrow p(i, A_\nu^2, A_\nu)$
        $\chi(i, A_\nu) \leftarrow \chi(i, A_\nu^2, A_\nu)$
else
    Calculate the cost $\chi(i, A_\nu)$ of path $p(i, A_\nu)$
Step 2
Find the shortest path from point B_ν to node j
if there are several same length shortest paths between B_ν and j **then**
    Select two paths: $p(B_\nu, B_\nu^1, j)$ and $p(B_\nu, B_\nu^2, j)$ where B_ν^1 and B_ν^2 are the intersection points of X and Y coordinates
    Calculate costs $\chi(B_\nu, B_\nu^1, j)$ and $\chi(B_\nu, B_\nu^2, j)$ of paths $p(B_\nu, B_\nu^1, j)$ and $p(B_\nu, B_\nu^2, j)$
    if $\chi(B_\nu, B_\nu^1, j) \leq \chi(B_\nu, B_\nu^2, j)$ **then**
        $p(B_\nu, j) \leftarrow p(B_\nu, B_\nu^1, j)$
        $\chi(B_\nu, j) \leftarrow \chi(B_\nu, B_\nu^1, j)$
    else
        $p(B_\nu, j) \leftarrow p(B_\nu, B_\nu^2, j)$
        $\chi(B_\nu, j) \leftarrow \chi(B_\nu, B_\nu^2, j)$
else
    Calculate the cost $\chi(B_\nu, j)$ of path $p(B_\nu, j)$
Step 3
Find the shortest path $p(A_\nu, B_\nu)$, on the border of zone ν, from point A_ν to nearest point (B_ν) of zone ν to node j
Let the cost $\chi(A_\nu, B_\nu)$ of path $p(A_\nu, B_\nu)$
Step 4
$p_\nu \leftarrow p(i, A_\nu) + p(A_\nu, B_\nu) + p(B_\nu, j)$
$\chi_\nu \leftarrow \chi(i, A_\nu) + \chi(A_\nu, B_\nu) + \chi(B_\nu, j)$
Return p_ν and χ_ν

5. Computational experiments and analyses

We now present the results of our computational experiments. All experiments were conducted on a server with one gigabyte RAM and an Intel Xeon 2.6 GHz processor. The P-L-HALNS was implemented in C++. We used CPLEX 12.6 with its default settings as the optimizer to solve the integer programming formulation.

In generating the instances, we assume an area divided into three nested squares centered in the middle of the area, each corresponding to a fixed speed zone, as shown in Fig. 3. The fixed speeds are set at 25, 32 and 40 km/h and the sizes of the nested squares are 3 km × 3 km, 6 km × 6 km and 10 km × 10 km, respectively. We assume a grid of Taxicab geometry with a distance of 100 m between each pair of neighboring points (starting from the bottom left corner) on each axis in the Cartesian plane. We generated four sets of instances where the first set contains 25 customers and four potential depots locations, the second set contains 50 customers and six potential depots locations, the third set contains 75 customers and eight potential depots locations, and the fourth set contains 100 customers and 10 potential depots. Each set includes three subsets: (1) customers concentrated in the city center, denoted by CC, (2) customers concentrated in the outer city area and in the suburb, denoted by SU, and (3) customers located randomly, denoted by R. These three subsets of benchmark instances are illustrated in Fig. 5. These configurations cover a wide variety of realistic urban settings.

Each subset includes five instances, resulting in a total of 60 instances. To generate the depot characteristics, we used a procedure similar to that used for the standard LRP benchmark instances (see Barreto, 2004; Albareda-Sambola et al., 2005; Prodhon, 2006). The customer demands and the depot capacities (in kg) were randomly generated using a uniform distribution in the range [100, 1100] and [10000, 15000], respectively. The fixed depot costs are dependent on their location (see Ghiani et al., 2013; Speh, 2009), i.e., zone 1 has the highest fixed cost (£5000/day per depot), followed by zone 2 (£3500/day per depot) and finally zone 3 (£2000/day per depot). All costs relate to the same planning horizon.

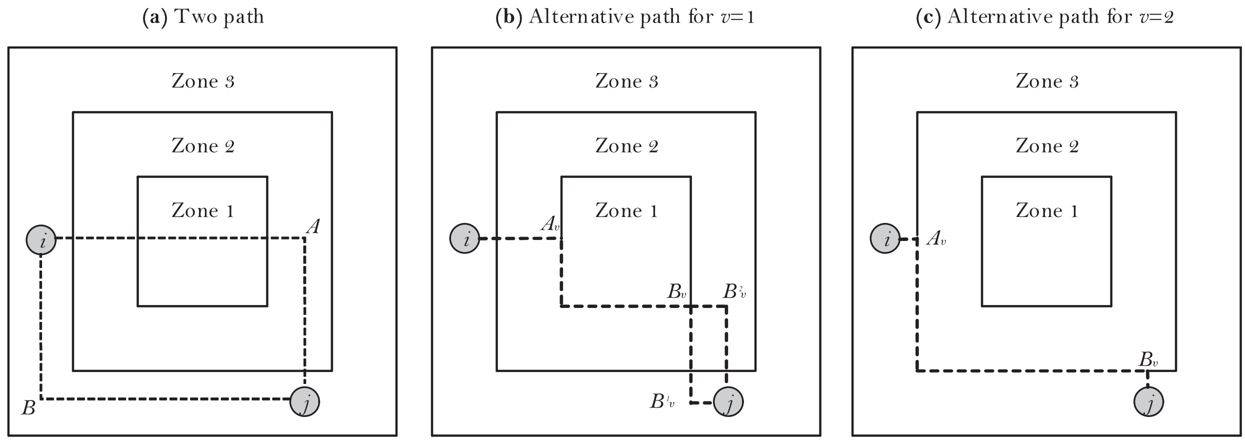

Fig. 4. Illustration of the three main steps of the Cheapest Path Calculation procedure.

Algorithm 4 General framework of the P-L-HALNS.

Fixed cost calculation: Calculate the fixed costs $\upsilon_{ij}^{\beta h}$
Initialization: Generate an initial solution
Initialize probabilities associated with the operators
$T \leftarrow c(\omega_0)P_0$, $q \leftarrow 1$, $p \leftarrow 1$, $l \leftarrow 1$, $\omega_c \leftarrow \omega_b \leftarrow \omega_0$
while $q < \varpi$ **do**
  if $l = \sigma$ **then**
    Diversification based destroy
    $l \leftarrow 1$
  else
    Intensification based destroy
    $l \leftarrow l + 1$
  Repair
  if $p = \varsigma$ **then**
    Calculate real costs
    $p \leftarrow 1$
  else
    Calculate the solution cost using fixed costs $\upsilon_{ij}^{\beta h}$
    $p \leftarrow p + 1$
  if $c(\omega_t) < c(\omega_c)$ **then**
    $\omega_c \leftarrow \omega_t$
  else
    $\vartheta \leftarrow e^{-(c(\omega_t)-c(\omega_c))/T}$
  Generate a random number ϵ
  if $\epsilon < \vartheta$ **then**
    $\omega_c \leftarrow \omega_t$
  if $c(\omega_c) < c(\omega_b)$ **then**
    $\omega_b \leftarrow \omega_c$
  $T \leftarrow \delta T$
  AWAP: update probabilities of operators
  $q \leftarrow q + 1$
end while

The parameters used in the P-L-HALNS are provided in Table 3. All algorithmic parametric values, except ς and σ, are as described in Demir et al. (2012), who applied an extensive meta-calibration procedure to generate effective parameter values for their ALNS heuristic for the PRP. In the experiments, ten runs were performed for each instance and the result of the best one is reported.

To empirically assess the quality of the approximation used to calculate the route lengths, we compare two versions of the P-L-HALNS. Version 1 corresponds to the original P-L-HALNS which uses average route demand lengths, while Version 2 uses actual costs at each iteration. We present two sets of experiments on selected 100-customer instances: CC100_1,

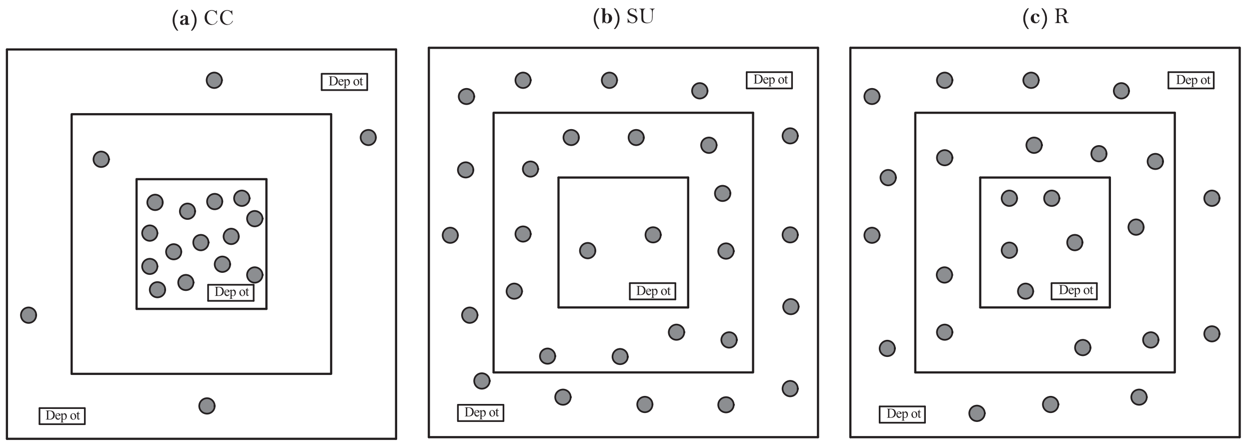

Fig. 5. Geographical customer distribution in the benchmark instances.

Table 3
Parameters used in the P-L-HALNS.

Description	Typical values
Total number of iterations (ϖ)	25,000
Number of iterations for roulette wheel (ζ)	450
Startup temperature parameter (P_0)	100
Cooling parameter (δ)	0.999
Lower limit of removable nodes	5–20% of $|\mathcal{N}_c|$
Upper limit of removable nodes	12–30% of $|\mathcal{N}_c|$
Route cost calculation parameter (ς)	100
Diversification parameter (σ)	50

Table 4
Sensitivity analyses of the P-L-HALNS components.

Instance	$|\mathcal{N}_c|$	$|\mathcal{N}_0|$	Version 1		Version 2		Dev_{TC}	Dev_T
			Total cost (£)	Time (s)	Total cost (£)	Time (s)		
CC100_1	100	10	21084.52	169.51	21090.52	231.55	0.03	26.79
SU100_1	100	10	15322.76	151.15	15324.86	201.17	0.01	24.86
R100_1	100	10	14028.78	158.13	14030.78	245.20	0.01	35.51
Avg (%)							0.01	29.06

SU100_1 and R100_1. The columns display the instance type, the total cost in (£) and the computation time in seconds (Time). The results are reported in Table 4. The columns Dev_{TC} and Dev_T show the percentage deterioration in solution quality and in computation time of Version 2 with respect to Version 1. The last row named Avg (%) shows the average deviations across the three instances. These results clearly indicate the benefit of using average route demand lengths (Version 1) in the P-L-HALNS. In terms of computation time, Version 2 performs on average 29.06% worse than Version 1. The solution costs between the two versions differ by 0.01% on average.

The rest of this section presents the full experiments, the aim of which is sevenfold: (1) to validate the heuristic in terms of accuracy, (2) to solve the problem described in Section 3, (3) to empirically calculate the savings that achievable by using a comprehensive objective function instead of using individual functions for each performance indicator, (4) to analyze the effect of variations in potential depot locations and customer distribution, (5) to investigate the effect of variations in depot costs, (6) to quantify the benefits of using a heterogeneous fleet over a homogeneous one, and (7) to analyze the arc-based network structure.

5.1. Validation test

We have conducted a preliminary experiment on small-size instances, aimed at assessing the accuracy of the P-L-HALNS. To this end, we have compared the solution values of our heuristic with the optimal values obtained by solving the integer programming formulation by CPLEX. We have generated five 10-customer instances, five 15-customer instances and five 20-customer instances, with three potential depots and two vehicle types, L1 and L2. Three values of demands, 500, 1000 or 1500 kg, were randomly assigned to each customer. We used a network in which the speeds are arc-dependent. We computed the fuel and CO_2 emission cost $c(i, j, f_{ij}^h)$ a priori for each arc $(i, j) \in \mathcal{A}$, for each vehicle type $h \in \mathcal{H}$ and for

Table 5
Computational results on the 10-,15 and 20-customer instances.

Instance	$\vert\mathcal{N}_c\vert$	$\vert\mathcal{N}_0\vert$	CPLEX		P-L-HALNS	
			Total cost (£)	Time (s)	Dev_T	Time (s)
ARC10_1	10	3	298.74	1.21	0.00	9.05
ARC10_2	10	3	300.32	0.77	0.00	6.25
ARC10_3	10	3	300.15	0.81	0.00	7.05
ARC10_4	10	3	299.14	2.18	0.00	7.90
ARC10_5	10	3	298.79	0.82	0.00	8.60
Avg			299.43	1.16	0.00	7.77
ARC15_1	15	3	2604.13	7.08	0.00	22.80
ARC15_2	15	3	2106.09	9.63	0.00	24.10
ARC15_3	15	3	2649.13	36.61	0.00	21.90
ARC15_4	15	3	2605.19	5.57	0.00	21.85
ARC15_5	15	3	2605.22	65.42	0.00	20.05
Avg			2513.95	24.86	0.00	22.14
ARC20_1	20	3	2699.45	1031.39	0.00	28.40
ARC20_2	20	3	2657.22	2739.87	0.00	29.05
ARC20_3	20	3	2649.72	489.18	0.00	27.45
ARC20_4	20	3	2649.92	3531.00	0.00	30.20
ARC20_5	20	3	2657.17	1008.88	0.00	29.85
Avg			2662.70	1760.06	0.00	28.99

Table 6
Average results on the instances.

Instance	$\vert\mathcal{N}_c\vert$	$\vert\mathcal{N}_0\vert$	Opened depots	Total distance (km)	CO_2 emissions (kg)	Fuel and CO_2 emissions costs (£)	Depot cost (£)	Vehicle cost (£)	Total cost (£)	Time (s)
CC25	25	4	(1.2, 0.2,0.5)	37.40	21.56	13.01	7900.00	106.20	8019.21	5.46
SU25	25	4	(0.4,0.8,0.6)	56.01	20.63	12.45	5400.00	102.60	5515.05	5.44
R25	25	4	(0.4,0.8,0.4)	64.78	19.48	11.76	5600.00	104.00	5715.76	5.41
CC50	50	6	(1.6,0.6,0.8)	80.66	23.68	14.29	11700.00	175.60	11889.88	32.11
SU50	50	6	(0.4,0.6,2.0)	125.15	21.44	12.94	8100.00	175.60	8288.53	31.00
R50	50	6	(0.2,1.0,1.8)	128.60	23.40	14.12	8100.00	169.00	8283.12	31.53
CC75	75	8	(2.2,1.0,0.8)	106.14	28.43	17.16	16100.00	256.80	16373.96	68.21
SU75	75	8	(0.0,2.0,2.0)	200.39	32.73	19.75	11300.00	288.80	11608.54	64.29
R75	75	8	(0.0,2.2,1.8)	197.89	38.22	23.06	11000.00	300.00	11323.04	64.02
CC100	100	10	(2.6,1.4,1.4)	140.24	43.61	26.31	20700.00	358.20	21084.52	169.51
SU100	100	10	(0.0,2.2,3.0)	244.44	42.02	25.35	14900.00	397.40	15322.76	151.15
R100	100	10	(0.0,3.0,2.2)	259.42	54.66	32.98	13600.00	395.80	14028.78	158.13

each possible load value. For example, consider three customers with having a demand of 500, 1000 and 1500, respectively. The total customer demand is 3000. We then calculate $c(i, j, f_{ij}^h)$ for the following six load values: 500, 1000, 1500, 2000, 2500 and 3000. Each instance was solved five times with the P-L-HALNS, and once with CPLEX. The results are shown in Table 5. The P-L-HALNS time is the total time needed for the five runs of the heuristic. These results clearly indicate that our heuristic always yields optimal solutions on these instances within short computation times.

5.2. Results obtained on the test instances

This section presents the results obtained by P-L-HALNS on the 25-, 50-, 75- and 100-customer instances. Table 6 presents the average results for each instance set where the columns display the average distance (km), CO_2 emissions (kg), fuel and CO_2 emissions cost (£), depot cost (£), vehicle cost (£), total cost (£) and time (s). We also report the average number of opened depots for each subset. In this column, the first, second and third elements within the parentheses represent the number of opened depots in zones 1, 2 and 3, respectively. To evaluate the environmental impact of the solutions, we also report the average amount of CO_2 emissions (in kg) based on the assumption that 1 L of gasoline contains 2.32 kg of CO_2 (Coe, 2005). For detailed results, the reader is referred to Tables A.1–A.4 in the Appendix.

From Table 6, it is clear that the total cost is dominated by the large depot costs which force the P-L-HALNS to first minimize the number of depots, then minimize the vehicle fixed costs, and lastly fuel and CO_2 emission costs.

5.3. The effect of the various cost components of the objective function

In this section, we analyze the implications of using different objectives on a number of performance measures. To this end, we have conducted experiments using four special cases of the objective function, which are presented in the first

Table 7
The effect of cost components: objective function values.

Objective	Opened depots	Total distance (km)	CO_2 emissions (kg)	Fuel and CO_2 emissions costs (£)	Depot cost (£)	Vehicle cost (£)	Total cost (£)
R100 instances							
Fuel and CO_2 emissions cost (*F*)	(1.0,3.1,1.0)	257.66	30.50	18.40	16443.79	363.51	16889.10
Depot cost (*D*)	(0.0,3.1,2.2)	238.34	52.41	31.63	13600.00	399.97	14030.00
Vehicle fixed cost (*V*)	(1.1,3.2,2.1)	248.40	36.34	21.93	18289.66	356.22	18666.46
Distance and vehicle fixed cost (DV)	(4.0,3.1,3.2)	333.19	119.59	72.17	34234.48	962.42	35263.31
Total cost (*T*)	(0.0,3.0,2.2)	259.42	54.66	32.98	13600.00	395.80	14028.78
SU100 instances							
Fuel and CO_2 emissions cost (*F*)	(1.1,3.0,2.0)	244.44	42.02	25.35	20037.93	416.03	20480.95
Depot cost (*D*)	(0.0,3.2,3.0)	304.11	43.62	26.32	16955.17	498.82	17480.01
Vehicle fixed cost (*V*)	(1.0,3.1,2.0)	250.09	62.91	37.96	20037.93	361.18	20438.29
Distance and vehicle fixed cost (DV)	(4.0,3.2,3.1)	340.56	92.48	55.81	37506.90	999.71	38562.30
Total cost (*T*)	(0.0,2.2,3.0)	248.49	43.52	26.26	14900.00	397.40	15322.76
CC100 instances							
Fuel and CO_2 emissions cost (*F*)	(3.0,2.0,1.1)	117.68	36.15	21.82	22080.00	369.49	22494.35
Depot cost (*D*)	(3.1,1.2,2.1)	161.18	69.36	41.85	20700.00	408.49	21140.94
Vehicle fixed cost (*V*)	(3.0,2.2,1.1)	124.22	43.97	26.53	22080.00	358.20	22467.62
Distance and vehicle fixed cost (DV)	(4.3,3.1,3.0)	256.51	86.30	52.08	33580.00	991.46	34579.22
Total cost (*T*)	(2.6,1.4,1.4)	140.24	43.61	26.31	20700.00	358.20	21084.52

Table 8
The effect of cost components: percent deviation from the minimum value.

Objective	Total distance (km)	CO_2 emissions (kg)	Fuel and CO_2 emissions costs (£)	Depot cost (£)	Vehicle cost (£)	Total cost (£)
R100 instances						
Fuel and CO_2 emissions cost (*F*)	8.11	0.00	0.00	20.91	2.05	20.39
Depot cost (*D*)	0.00	71.86	71.86	0.00	12.28	0.01
Vehicle fixed cost (*V*)	4.22	19.15	19.15	34.48	0.00	33.06
Distance and vehicle fixed cost (DV)	39.79	292.13	292.13	151.72	170.18	151.36
Total cost (*T*)	8.84	79.22	79.21	0.00	11.11	0.00
SU100 instances						
Fuel and CO_2 emissions cost (*F*)	0.00	0.00	0.00	18.18	15.19	33.66
Depot cost (*D*)	24.41	3.82	3.82	0.00	38.11	14.08
Vehicle fixed cost (*V*)	2.31	49.73	49.73	18.18	0.00	33.39
Distance and vehicle fixed cost (DV)	39.32	120.12	120.12	121.21	176.79	151.67
Total cost (*T*)	1.66	3.57	3.57	0.00	10.03	0.00
CC100 instances						
Fuel and CO_2 emissions cost (*F*)	0.00	0.00	0.00	6.67	3.15	6.69
Depot cost (*D*)	36.97	91.85	91.85	0.00	14.04	0.27
Vehicle fixed cost (*V*)	5.56	21.63	21.63	6.67	0.00	6.56
Distance and vehicle fixed cost (DV)	117.97	138.73	138.73	62.22	176.79	64.00
Total cost (*T*)	19.18	20.62	20.62	0.00	0.00	0.00

column of Table 7. The tests were run on all 100-customer R, SU and CC instances. In the first version, we only consider minimizing the fuel and CO_2 emissions costs (*F*). This setting also implies minimizing CO_2 since emissions are proportional to fuel consumption. We then consider the objective of minimizing only the depot cost (*D*) and the vehicle fixed cost (*V*) in the second and third versions, respectively. The next objective corresponds to that of the HVRP which jointly minimizes distance and vehicle fixed costs (DV). Finally, we present the comprehensive objective of minimizing the total cost function (*T*) as defined by (7).

Table 8 presents the average deviations of each component from the smallest value of each column. For example, in the case of the R100 instances, the minimum average value for objective *D* is £13,600 across the five objective functions, but objective *V* yields a solution in which the average depot cost is £18,289.66, corresponding to an increase of 34.48% over the former. For the R100, SU100 and CC100 instances, it is clear that objective *F* results in a poor total cost performance, yielding a 20.39%, 33.66% and 6.69% average increases over the value found through objective *T*, respectively. In the case of the R100 instances, this increase is more substantial for objective *V*, which is on average 33.06% higher. For the R100, SU100 and CC100 instances, as for emissions, objective *F* yields an increase of 20.91%, 18.18% and 6.67% in depot cost over the value provided by objective *D*, respectively. For the R100, SU100 and CC100 instances, objective DV performs very poorly on all cost components, yielding average increases of 151.36%, 151.67% and 64.00%, respectively. These results indicate that traveling on a shortest path does not always result in a cheapest solution. In urban settings, due to the effect of speed zones on the objective function, longer paths outside the city center have the potential to decrease the solution cost, a situation that was explained in Section 2. Maden et al. (2010) reached a similar conclusion relative to long-haul transportation.

Table 9
The effect of variations in depot location over different customer positionings.

Instance	All depots in zone 1				All depots in zone 2				All depots in zone 3				Base case	
	CO_2 (kg)	Total cost (£)	Dev_{CO_2}	Dev_T	CO_2 (kg)	Total cost (£)	Dev_{CO_2}	Dev_T	CO_2 (kg)	Total cost (£)	Dev_{CO_2}	Dev_T	CO_2 (kg)	Total cost (£)
R100_1	110.68	25390.30	3.45	41.14	90.10	17866.20	−18.60	16.35	77.36	10367.00	−38.12	−44.15	106.86	14944.50
R100_2	52.29	25464.60	16.50	47.34	43.26	17917.10	−0.93	25.15	40.40	10461.00	−8.06	−28.19	43.66	13410.30
R100_3	50.77	25421.60	14.23	47.19	38.62	17907.30	−12.75	25.03	40.77	10422.60	−6.82	−28.80	43.55	13424.30
R100_4	54.14	25465.70	21.44	47.34	40.92	17946.70	−3.94	25.28	38.28	10488.10	−11.12	−27.86	42.53	13409.70
R100_5	77.70	25388.90	52.80	41.10	35.66	17866.50	−2.86	16.30	35.20	10366.30	−4.20	−44.27	36.68	14955.10
Avg (%)			21.68	44.82			−7.82	21.62			−13.66	−34.65		
CC100_1	37.20	27969.60	8.06	18.23	33.20	24869.60	−3.01	8.04	31.20	19869.60	−9.62	−15.10	34.20	22869.60
CC100_2	39.67	24844.10	7.64	28.10	35.64	21061.10	−2.81	15.18	32.64	14994.10	−12.26	−19.14	36.64	17864.10
CC100_3	77.06	29473.30	9.08	23.89	68.06	24753.30	−2.94	9.37	65.06	20433.30	−7.69	−9.79	70.06	22433.30
CC100_4	41.36	30883.10	7.50	25.90	36.26	25183.10	−5.52	9.13	34.26	20783.10	−11.68	−10.10	38.26	22883.10
CC100_5	42.88	26378.50	9.33	26.56	36.88	22092.50	−5.42	12.31	34.88	16872.50	−11.47	−14.82	38.88	19372.50
Avg (%)			8.32	24.54			−3.94	10.81			−10.54	−13.79		
SU100_1	51.44	23939.00	19.44	37.72	40.44	16919.00	−2.47	11.88	37.44	10909.00	−10.68	−36.67	41.44	14909.00
SU100_2	54.71	24962.40	20.11	40.10	41.40	17552.40	−5.57	14.81	36.71	10152.40	−19.07	−47.28	43.71	14952.40
SU100_3	47.64	22976.30	18.89	34.91	36.54	16906.30	−5.75	11.53	31.64	10956.30	−22.12	−36.51	38.64	14956.30
SU100_4	55.68	26887.00	19.76	37.19	43.68	18987.00	−2.29	11.06	37.68	12787.00	−18.58	−32.06	44.68	16887.00
SU100_5	50.61	25809.10	17.78	42.23	39.61	16609.10	−5.05	10.24	33.61	10909.10	−23.81	−36.67	41.61	14909.10
Avg (%)			19.20	38.43			−4.23	11.90			−18.85	−37.84		

5.4. The joint effect of variations in depot and customer locations

In this section, we investigate the joint effect of the variations in potential depot locations and customer distribution in two sets of experiments. In the first set, we have selected instances with 100 customers and 10 potential depots. We consider three depot location variations, namely all depots are potentially located in zone 1, in zone 2, and in zone 3, respectively. We also consider three customer location variations, i.e., R, CC and SU type instances. In total, we have generated nine sets of depot and customer location combinations. In the tables, the columns Dev_{CO_2} and Dev_T show the deviations in CO_2 emissions (in kg) and in total cost (£) between the various depot or customer location cases and the base case.

We report the effect of varying the depot location over different customer location in Table 9. For the R instances, Table 9 shows that when all depots are located in zone 1, CO_2 emissions increase by 21.68%. When they are located in zones 2 and 3, CO_2 emissions decrease by 7.82% and 13.66%, respectively. Table 9 suggests that the average increase in the total cost is 44.82% and 21.62% over the base case, when all depots are located in zones 1 and 2, respectively. When all the depots are located in zone 3, the total cost decreases by about 34.65% on average. For the CC instances, Table 9 shows that when all depots are located in zone 1, CO_2 emissions increase on average by 8.32% because of the customers that are not located in the city center. In this case, the vehicles must visit these outlying customers and return to a depot located in zone 1, which increases fuel consumption and CO2 emissions. On the other hand, the emissions decrease by 3.94% and 10.54% when customers are located in zones 2 and 3, respectively. The average increase in the total cost is 24.54% and 10.81% on average when all depots are located in zones 1 and 2, respectively. The total cost decreases by 13.79% on average when all the depots are located in zone 3. For the SU instances, similar results obtained as for the R instances. When all depots are located in zone 1, CO_2 emissions increase on average by 19.20% and decrease by 4.23% and 18.85% when they are located in zones 2 and 3, respectively. The total cost increases by 38.43% and 11.90% on average when all depots are located in zones 1 and 2, respectively. The total cost decreases by 37.84% on average when all the depots are located in zone 3. For all types of instances, i.e., R, CC, SU, this analysis indicates that in terms of cost, it is preferable to locate the depots in suburban areas rather than in the city center. This also helps reduce congestion in city centers. A similar observation was made by Dablanc et al. (2014) who conducted an empirical study on depot location in the Los Angeles area and concluded that warehouses moved out an average of six miles from the area barycenter between 1998 and 2009. Dablanc's findings are mainly a consequence of the fact that land is cheaper in the suburbs than in inner-cities, which translates into lower depot costs. Our study goes one step further in that it shows that locating depots in peripheral zones also helps reduce pollution since more travel can be made at an optimal speed. Locating depots outside the city center translates into larger driving distances to the inner city customers but yields overall economic and environmental benefits.

In the second set of experiments, we analyze the effect of variations in customer locations. Table 10 provides a comparison of three variations, namely all customers located in zone 1, all customers located in zone 2, and all customers located in zone 3. The depot locations are kept the same across all variations. Table 10 shows that when all customers are located in zone 3, CO_2 emissions increase by 11.42%. On the other hand, when all customers are located in zones 1 and 2, CO_2 emissions decrease by 38.97% and 50.14%, respectively. Table 10 suggests that the average total cost increase over the base case is 38.16%, 6.04% and 8.12% on average when all customers are located in zones 1, 2 and 3, respectively. For the case where all customers are located in zones 1, 2 and 3, the increase in the total cost ranges from 33.25% to 41.50%, from −0.33% to

Table 10
The effect of variations in customer location.

Instance	All customers in zone 1				All customers in zone 2				All customers in zone 3				Mix	
	CO_2 (kg)	Total cost (£)	Dev_{CO_2}	Dev_T	CO_2 (kg)	Total cost (£)	Dev_{CO_2}	Dev_T	CO_2 (kg)	Total cost (£)	Dev_{CO_2}	Dev_T	CO_2 (kg)	Total cost (£)
R100_1	63.66	22411.30	−67.86	33.32	65.15	14906.20	−64.02	−0.26	107.55	14912.70	0.64	−0.21	106.86	14944.50
R100_2	29.63	22877.90	−47.35	41.38	27.18	14938.40	−60.61	10.23	46.55	14950.10	6.22	10.30	43.66	13410.30
R100_3	30.66	22878.50	−42.02	41.32	25.80	14948.60	−68.83	10.20	47.04	14954.40	7.42	10.23	43.55	13424.30
R100_4	33.76	22922.40	−25.98	41.50	40.16	14959.30	−5.92	10.36	54.87	16882.10	22.48	20.57	42.53	13409.70
R100_5	32.85	22406.20	−11.66	33.25	24.24	14905.60	−51.34	−0.33	46.05	14911.80	20.35	−0.29	36.68	14955.10
Avg (%)			−38.97	38.16			−50.14	6.04			11.42	8.12		

Table 11
The effect of same depot costs on opened depots.

Instance	£5000 Opened depots	£3500 Opened depots	£2000 Opened depots	£1000 Opened depots	£500 Opened depots	Mix Opened depots
R100_1	(2,3,0)	(2,3,0)	(2,3,0)	(1,3,1)	(1,3,1)	(0,3,2)
R100_2	(2,3,0)	(1,3,1)	(1,3,1)	(2,2,1)	(1,3,1)	(0,3,2)
R100_3	(2,3,0)	(1,3,1)	(1,3,1)	(1,3,1)	(1,3,1)	(0,3,2)
R100_4	(1,3,1)	(1,3,1)	(2,2,2)	(1,3,2)	(2,2,2)	(0,3,3)
R100_5	(1,3,1)	(1,3,1)	(1,3,1)	(1,3,1)	(1,3,1)	(0,3,2)
Avg	(1.6,3.0,0.4)	(1.2,3.0,0.8)	(1.4,2.8,1.0)	(1.2,2.8,1.2)	(1.2,2.8,1.2)	(0.0,3.0,2.2)

10.36%, and from −0.29% to 20.57%, respectively. Our results suggest that when all customers are located only in the city center this is always more expensive than for the other settings.

5.5. The effect of variations in depot costs

In practice, it is very difficult to estimate depot costs because these depend on factors such as land and building cost, staffing and technology. In general, these factors are highly variable and hard to quantify. In our benchmark instances, the depot costs are high with respect to other costs and dependent on their location, i.e., every zone has its own fixed depot cost. We now investigate the effect of variations in depot costs.

Our first experiments analyze the effect of same depot costs on opened depots. To this end, we have selected five R type instances with 100 customers and 10 depots. We consider five versions in which all depot costs are fixed at £5000, £3500, £2000, £1000 and £500 per day in all zones. Table 11 shows that when the variable depot cost (Mix) is used for each zone, 5.5 depots are opened in zones 2 and 3 on average. For the £5000, £3500, £2000, £1000 and £500 fixed costs, 3.4, 3.8, 3.8, 4.0 and 4.0 depots are opened in zones 2 and 3 on average. On the other hand, for these three fixed costs variants, 1.6, 1.2, 1.4, 1.2 and 0.0 depots are opened in zone 1 on average. The average number of opened depots in the city center is always lower than the total of number of opened depots in the outer urban area and in the suburb. Our results clearly show that even if depot costs are the same in everywhere, it is still preferable to locate depots outside the city center because of the pollution aspect (see Section 5.4).

Our next experiments investigate the effect of decreasing the variable depot costs. To this end, we have conducted four series of tests on all 100-customer CC, SU and R instances using our original variable depot costs structure. In these tests, we decrease the depot costs by 90%, 70%, 50% and 30%, respectively. For example, decreasing the depot cost by 90% means that the depot costs in zones 1, 2 and 3 are £500, £350 and £200, respectively. Looking at the results presented in Table 12, we observe no change in the locations of opened depots for all instances and for all variations. For example, for the CC100 instances, when we decrease depot costs by 90%, 70%, 50% and 30%, it is still preferable to open three depots in zone 1, one depot in zone 2 and two depots in zone 3. Even though customers are concentrated in the city center, half of the depots are still located in the suburb. When we look at the SU100 instances, no depot is located in city center, but six depots are located in outer city area and in the suburb. The R100 instances follows the same pattern with no depot located in the city center, but five depots located in the outer city area and in the suburb. Again, these results clearly show that no matter what the depot cost is, it is still preferable to locate the depots outside the city center due to the impact of their location on CO_2 emissions.

5.6. The effect of fleet composition

This section analyzes the benefit of using a heterogeneous fleet of vehicles over a homogenous one. To this end, we have conducted three sets of experiments on 100-customer instances, each using a unique vehicle type, i.e., only light duty 1 (L1), only light duty 2 (L2) and only medium duty (M). This results in three instances of the homogeneous version of the problem which are solved with the P-L-HALNS. Table 13 provides the results of this comparison. The columns Dev_{CO_2} and Dev_T show

Table 12
The effect of decreasing the depot costs.

Instance	Change in depot cost (%)	Opened depots	Total distance (km)	CO_2 emissions (kg)	Fuel and CO_2 emissions costs (£)	Depot cost (£)	Vehicle cost (£)	Total cost (£)
CC100	−90%	(3,1,2)	106.74	63.93	38.58	2070.00	358.20	2424.02
SU100	−90%	(0,3,3)	255.71	24.29	14.66	1695.52	372.56	2080.63
R100	−90%	(0,3,2)	250.70	34.63	20.90	1360.00	395.80	1756.22
CC100	−70%	(3,1,2)	155.11	71.33	43.05	6210.00	358.20	6576.01
SU100	−70%	(0,3,3)	268.67	45.66	27.56	5086.55	372.56	5485.30
R100	−70%	(0,3,2)	279.48	25.98	15.68	4080.00	407.26	4479.27
CC100	−50%	(3,1,2)	129.82	66.44	40.09	10350.00	358.20	10722.59
SU100	−50%	(0,3,3)	239.59	44.95	27.12	8477.59	372.56	8876.44
R100	−50%	(0,3,2)	258.55	54.19	32.70	6800.00	395.80	7222.50
CC100	−30%	(3,1,2)	115.79	60.75	36.66	14490.00	358.20	14868.95
SU100	−30%	(0,3,3)	247.62	13.93	8.41	11868.62	372.56	12249.06
R100	−30%	(0,3,2)	253.99	52.10	31.44	9520.00	399.97	9946.26

Table 13
The effect of using a heterogeneous fleet.

Instance	Only light duty 1				Only light duty 2				Only medium duty				Heterogeneous fleet	
	CO_2 (kg)	Total cost (£)	Dev_{CO_2}	Dev_T	CO_2 (kg)	Total cost (£)	Dev_{CO_2}	Dev_T	CO_2 (kg)	Total cost (£)	Dev_{CO_2}	Dev_T	CO_2 (kg)	Total cost (£)
CC100_1	50.12	26286.20	46.55	14.94	28.56	23007.20	−16.48	0.60	29.33	22877.70	−14.22	0.04	34.20	22869.60
CC100_2	51.80	22745.30	41.40	27.32	35.47	21011.40	−3.19	17.62	32.82	19379.80	−10.43	8.48	36.64	17864.10
CC100_3	71.24	26251.50	1.69	17.02	55.17	22508.80	−21.25	0.34	55.14	22441.20	−21.29	0.04	70.06	22433.30
CC100_4	46.78	24784.20	22.27	8.31	39.50	23013.80	3.24	0.57	35.77	22981.60	−6.52	0.43	38.26	22883.10
CC100_5	52.06	22745.40	33.91	17.41	33.04	22509.90	−15.02	16.20	35.08	19441.20	−9.77	0.35	38.88	19372.50
Avg (%)			29.16	17.00			−10.54	7.06			−12.45	1.87		
SU100_1	40.33	17280.30	−2.67	15.91	35.31	17011.30	−14.78	14.10	42.59	16885.70	2.77	13.26	41.44	14909.00
SU100_2	34.32	15234.70	−21.48	1.89	32.66	14960.70	−25.28	0.06	41.37	15445.00	−5.36	3.29	43.71	14952.40
SU100_3	41.72	15739.20	7.96	5.23	35.59	15511.50	−7.90	3.71	43.12	15446.00	11.60	3.27	38.64	14956.30
SU100_4	38.36	17295.10	−14.16	2.42	35.00	17511.10	−21.67	3.70	42.15	17445.40	−5.67	3.31	44.68	16887.00
SU100_5	35.40	15235.40	−14.92	2.19	29.83	15008.00	−28.31	0.66	42.67	14943.30	2.55	0.23	41.61	14909.10
Avg (%)			−9.05	5.53			−19.59	4.45			1.18	4.67		
R100_1	98.27	15237.10	−8.04	1.96	73.68	15010.30	−31.05	0.44	111.96	15145.30	4.77	1.34	106.86	14944.50
R100_2	38.89	15279.50	−10.92	13.94	34.67	15010.90	−20.59	11.94	44.55	15006.90	2.03	11.91	43.66	13410.30
R100_3	40.07	15280.20	−8.00	13.82	31.36	15008.90	−27.99	11.80	43.05	15004.20	−1.15	11.77	43.55	13424.30
R100_4	38.81	17279.40	−8.76	28.86	33.74	17010.40	−20.68	26.85	42.57	16885.70	0.09	25.92	42.53	13409.70
R100_5	36.10	15235.80	−1.57	1.88	32.49	14960.60	−11.41	0.04	40.59	15144.50	10.65	1.27	36.68	14955.10
Avg (%)			−7.46	12.09			−22.34	10.21			3.28	10.44		

the deviations in CO_2 emissions (in kg) and in total cost between the various homogeneous cases and the heterogeneous case.

Table 13 shows that for the CC instances, CO_2 emissions increase by 29.16% when L1 vehicles are used, and decrease by 10.54% and 12.45% when L2 and M vehicles are used, respectively. The results of the SU and R instances yield similar values for CO_2 emissions, which decrease by L1 and L2 vehicles and increase by M type vehicles. Table 13 indicates that the average increase in total cost for the CC instances is 17.00%, 7.06% and 1.87%, for the SU instances 5.53%, 4.45% and 4.67%, for the R instances 12.09%, 10.21% and 10.44% when using L1, L2 and M homogeneous fleet over the heterogeneous case, respectively. These results imply that if one is to use a homogeneous fleet, it is preferable to use vehicles of type M in city centers (CC). For the suburban (SU) and randomly distributed customer (R) location scenarios, homogeneous vehicles of types L2 and M yield almost the same average total cost increase. This result shows that both the L2 and M vehicles are suitable for the SU and R instances. Our results also show that using a heterogeneous vehicle fleet is preferable to using a homogeneous one since the total cost decreases by about at most 17%. For urban settings or short-haul transportation, using a heterogeneous fleet does not seem to have same impact on the total cost as in long-haul transportation. Koç et al. (2014) have indeed shown that using a heterogeneous fleet can decrease the total cost by up to 25% in inter-city travel.

Our final experiments aim at providing some insight into the capacity utilization of the vehicle fleet, both for the homogenous and the heterogeneous cases, and also into the capacity utilization of the depots. In Table 14, we present the capacity utilizations for the three homogeneous settings of Table 13 as well as for the heterogeneous version. The column DCU displays the average percentage of capacity utilization for depots, which is calculated as 100 (total demand of customers assigned to corresponding depot)/(capacity of the depot) for each depot, and the column VCU displays the average percentage capacity utilization of the vehicle fleet, which is calculated as 100 (total demand of route)/(capacity of the vehicle) for each vehicle.

Table 14
Capacity utilization rates.

Instance	Only light duty 1		Only light duty 2		Only medium duty		Heterogeneous fleet	
	DCU	VCU	DCU	VCU	DCU	VCU	DCU	VCU
CC100_1	91.67	90.40	89.16	86.79	92.98	86.79	89.16	92.98
CC100_2	96.39	90.72	99.50	82.26	93.47	82.26	97.92	92.77
CC100_3	87.92	93.09	97.39	84.40	97.39	72.35	97.39	85.54
CC100_4	88.76	92.46	99.36	88.76	91.19	88.76	91.19	88.76
CC100_5	96.86	92.59	98.38	83.95	96.86	71.96	93.97	89.94
Avg (%)	92.32	91.85	96.76	85.23	94.38	80.42	93.93	90.00
SU100_1	88.22	94.35	88.22	90.57	88.22	90.57	88.22	90.57
SU100_2	93.28	91.90	94.69	92.59	99.20	71.42	99.20	88.65
SU100_3	97.13	89.99	97.13	81.59	97.13	69.94	97.13	78.96
SU100_4	92.07	94.95	98.01	81.02	96.45	69.45	98.01	86.19
SU100_5	95.78	94.37	95.78	85.56	95.78	73.34	97.23	82.27
Avg (%)	93.30	93.11	94.77	86.27	95.36	74.94	95.96	85.33
R100_1	94.37	92.99	97.28	84.31	94.37	72.26	94.37	91.64
R100_2	98.18	91.36	98.18	87.71	98.18	65.78	98.18	88.30
R100_3	98.92	90.68	97.44	87.05	97.44	65.29	97.44	83.70
R100_4	86.76	92.79	86.76	89.08	86.76	89.08	86.76	89.08
R100_5	94.20	92.82	94.20	93.51	94.20	72.13	94.20	89.53
Avg (%)	94.49	92.13	94.77	88.33	94.19	72.91	94.19	88.45

Table 15
Computational results of the arc based network structure.

Instance	$\lvert\mathcal{N}_c\rvert$	$\lvert\mathcal{N}_0\rvert$	Total distance (km)	CO_2 emissions (kg)	Fuel and CO_2 emissions costs (£)	Depot cost (£)	Vehicle cost (£)	Total cost (£)	DCU	VCU	Time (s)
ARC100_1	100	10	126.97	119.09	71.87	3450.00	823.00	4344.87	87.37	72.37	149.53
ARC100_2	100	10	142.05	121.30	73.20	3650.00	910.00	4633.20	89.84	68.53	171.07
ARC100_3	100	10	127.19	116.62	70.37	3450.00	753.00	4273.37	86.94	72.59	172.89
ARC100_4	100	10	129.52	116.71	70.43	3650.00	896.00	4616.43	84.15	72.59	168.28
ARC100_5	100	10	114.19	110.69	66.80	3650.00	952.00	4668.80	88.29	74.67	161.76
Avg			127.98	116.88	70.53	3570.00	866.80	4507.33	87.32	72.15	164.71

As can be seen from Table 14, for the CC, SU and R instances the VCU reaches its maximum average level of 91.85%, 93.11% and 92.13% and its minimum average level of 80.42%, 74.94% and 72.91% when using only L1 and M duty vehicles, respectively. Using L1 vehicles yields the maximum average VCU level over all types of instances. Using a heterogeneous fleet yields an average VCU of 90.00%, 85.33% and 88.45% for the CC, SU and R instances, respectively. These results indicate that for a heterogeneous fleet, the best VCU is obtained with L1 vehicles for the CC instances, and with L2 vehicles for the SU or the R instances.

For all instance types and all homogeneous vehicle combinations, the DCU level reaches at least 92.00%, which is very similar to the heterogeneous vehicle fleet level. Our results show that because of the very high effect of the depot costs in the objective function (see Section 5.2), increasing the DCU has more effect than increasing the VCU in urban settings.

5.7. Application to an arc-based speed structure

We have so far almost exclusively assumed that speed zones corresponds to distinct geographic regions of the urban area, which is not always the case in a real-world urban setting. However, our analysis also applies to situations in which speeds are not zone-dependent, but arc-dependent. To illustrate, we now analyze a different network structure to further motivate the wide applicability of our model. To this end, we consider a network in which the speed limits are arc-specific attributes. We have generated five instances, ARC100_1, ARC100_2, ARC100_3, ARC100_4 and ARC100_5, containing 100 customers and 10 potential depots located randomly in the 10 km $\times$ 10 km square. We randomly assigned one of the three speed values, 25, 32 or 40 km/h, to each arc (i, j) and one of the three depot costs values, £500/day per depot, £350/day per depot or £200/day per depot. Table 15 presents the results of the arc-based speed structure on five instances. These results indicate that our algorithm work just as well with arc-dependent speeds. They also show that average values of CO_2 emissions are 116.88 kg, fuel and CO_2 emissions costs are £70.53, the depot cost is £3570.00, the vehicle cost is £866.80, and the total cost is £4507.33. Depot and vehicle utilization values are on average equal to 87.32% and 72.15%. As for speed zone-based networks, the total cost is largely dominated by depot costs. Due to this effect, the DCU is 15.17% higher than the VCU in urban settings.

6. Conclusions and managerial insights

We have studied and analyzed the combined impact of depot location, fleet composition and routing on vehicle emissions in city logistics. We have formulated a new problem arising in urban settings and designed a powerful ALNS metaheuristic to solve it. We have derived managerial insights by investigating the effect of various problem components on cost and CO_2 emissions. In what follows we summarize our main conclusions.

Our first observation relates to shortest paths. Because of the effect of speed zones, a shortest path is not always a fastest, cheapest or least polluting path in city logistics since it may be advantageous to follow circuitous routes to achieve faster speeds and hence lower costs and CO_2 emissions. The explanation lies in the fact that emissions are a U-shaped function of speed (Fig. 1) whose optimal value is reached at 40 km/h since this is the fastest speed used in this study. It is also often the maximal allowed speed in city centers. Hence faster driving is clearly cheaper and less polluting in this context. This is consistent with what was observed by Ehmke et al. (2014) for urban areas but different from what occurs in inter-city travel where faster driving entails more pollution which must be weighed against reduced driver wages (Bektaş and Laporte, 2011; Demir et al., 2014a).

We have also shown that the highest costs are attained when all customers are located only in the city center. Our experimental results indicate that even for same depot costs or lower variable depot costs, it is preferable to locate the depots outside the city center. This decreases the total cost by about 34.65% on average, a finding in line with that of Dablanc et al. (2014) on the Los Angeles data. We have further performed an extensive analysis of the interactions between customer distribution and depot location, and we have shown that this conclusion holds over a wide range of fixed depot costs and customer geographical distributions.

We have demonstrated that in an urban setting, using a heterogeneous fleet instead of a homogeneous one can decrease average costs by up to 17%, but this is not as much as the 25% reduction observed by Koç et al. (2014) for long-haul transportation. Furthermore, we have shown that the depot capacity utilization levels tend to be higher than the vehicle capacity utilization levels. This has an important implication since in practice depot costs are often considerably larger than vehicle costs and significantly affect the total distribution cost.

Our results depend of course on the parameter values used in the experimental design but the extensive sensitivity analyses we have carried out convince us that our conclusions are highly robust. Beyond the computational comparisons we have just made, we stress the importance of the availability of a flexible decision support tool, such as the one we have developed, capable of handling a wide variety of city configurations and of analyzing the trade-offs that can be established between depot location, fleet composition, routing and polluting emissions reductions in city logistics networks.

Acknowledgments

The authors gratefully acknowledge funding provided by the Southampton Business School at the University of Southampton and by the Canadian Natural Sciences and Engineering Research Council under Grants 2015-06189 and 436014-2013. Thanks are due to a referee who provided valuable advice on previous versions of this paper.

Appendix

Table A.1–A.4 present the detailed computational results on the 25-, 50-, 75- and 100-customer instances, respectively.

Table A.1
Computational results on the 25-customer instances.

Instance	$\lvert\mathcal{N}_c\rvert$	$\lvert\mathcal{N}_0\rvert$	P-L-HALNS							
			Opened depots	Total distance (km)	CO_2 emissions (kg)	Fuel and CO_2 emissions costs (£)	Depot cost (£)	Vehicle cost (£)	Total cost (£)	Time (s)
CC25_1	25	4	(1,1,0)	36.10	26.12	15.76	8500.00	109.00	8624.76	5.16
CC25_2	25	4	(2,0,0)	45.59	10.09	6.09	10000.00	109.00	10115.10	5.20
CC25_3	25	4	(1,0,1)	37.60	2.63	1.59	7000.00	102.00	7103.59	5.50
CC25_4	25	4	(1,0,1)	40.24	29.35	17.71	7000.00	109.00	7126.71	6.02
CC25_5	25	4	(1,0,1)	27.47	39.62	23.91	7000.00	102.00	7125.91	5.42
SU25_1	25	4	(0,1,1)	54.65	9.68	5.84	5500.00	102.00	5607.84	5.48
SU25_2	25	4	(1,0,1)	63.99	8.93	5.39	7000.00	109.00	7114.39	5.48
SU25_3	25	4	(0,1,0)	52.97	45.60	27.52	3500.00	98.00	3625.52	5.42
SU25_4	25	4	(1,1,0)	46.88	0.15	0.09	5500.00	102.00	5602.09	5.38
SU25_5	25	4	(0,1,1)	61.55	38.78	23.40	5500.00	102.00	5625.40	5.44
R25_1	25	4	(0,1,0)	73.07	28.63	17.28	3500.00	98.00	3615.28	5.36
R25_2	25	4	(0,1,1)	63.54	21.66	13.07	5500.00	102.00	5615.07	5.38
R25_3	25	4	(0,1,0)	68.13	10.17	6.14	3500.00	102.00	3608.14	5.36
R25_4	25	4	(1,1,0)	58.57	26.00	15.69	8500.00	109.00	8624.69	5.32
R25_5	25	4	(1,0,1)	60.58	10.95	6.61	7000.00	109.00	7115.61	5.62

Table A.2
Computational results on the 50-customer instances.

Instance	$\|\mathcal{N}_c\|$	$\|\mathcal{N}_0\|$	P-L-HALNS							
			Opened depots	Total distance (km)	CO_2 emissions (kg)	Fuel and CO_2 emissions costs (£)	Depot cost (£)	Vehicle cost (£)	Total cost (£)	Time (s)
CC50_1	50	6	(1,0,2)	92.86	20.74	12.52	9000.00	180.00	9192.52	33.56
CC50_2	50	6	(2,1,0)	70.76	19.83	11.97	13500.00	180.00	13692.00	33.80
CC50_3	50	6	(1,1,1)	75.47	36.37	21.94	10500.00	169.00	10690.90	31.08
CC50_4	50	6	(2,0,1)	77.13	21.10	12.73	12000.00	169.00	12181.70	31.14
CC50_5	50	6	(2,1,0)	87.07	20.34	12.27	13500.00	180.00	13692.30	30.97
SU50_1	50	6	(1,0,2)	144.13	24.37	14.71	10500.00	180.00	10694.70	30.92
SU50_2	50	6	(0,1,2)	134.87	41.57	25.08	7500.00	169.00	7694.08	30.93
SU50_3	50	6	(0,1,2)	123.49	1.76	1.06	7500.00	169.00	7670.06	31.30
SU50_4	50	6	(0,1,2)	123.17	20.70	12.49	7500.00	180.00	7692.49	30.85
SU50_5	50	6	(1,0,2)	100.09	18.79	11.34	7500.00	180.00	7691.34	31.00
R50_1	50	6	(1,1,1)	116.06	15.38	9.28	9000.00	169.00	9178.28	30.74
R50_2	50	6	(0,1,2)	133.68	21.97	13.26	7500.00	169.00	7682.26	31.62
R50_3	50	6	(0,1,2)	136.19	39.99	24.13	7500.00	169.00	7693.13	32.03
R50_4	50	6	(0,1,2)	131.86	19.17	11.57	7500.00	169.00	7680.57	31.16
R50_5	50	6	(0,1,2)	125.23	20.49	12.36	9000.00	169.00	9181.36	32.07

Table A.3
Computational results on the 75-customer instances.

Instance	$\|\mathcal{N}_c\|$	$\|\mathcal{N}_0\|$	P-L-HALNS							
			Opened depots	Total distance (km)	CO_2 emissions (kg)	Fuel and CO_2 emissions costs (£)	Depot cost (£)	Vehicle cost (£)	Total cost (£)	Time (s)
CC75_1	75	8	(2,1,1)	110.65	27.51	16.60	15500.00	240.00	15756.60	71.18
CC75_2	75	8	(2,1,1)	113.19	29.38	17.73	15500.00	282.00	15799.70	71.62
CC75_3	75	8	(2,1,1)	117.68	30.03	18.12	15500.00	240.00	15758.10	68.32
CC75_4	75	8	(3,1,0)	95.75	28.62	17.27	18500.00	282.00	18799.30	64.60
CC75_5	75	8	(2,1,1)	93.41	26.61	16.06	15500.00	240.00	15756.10	65.33
SU75_1	75	8	(0,2,2)	219.38	35.14	21.20	11000.00	320.00	11341.20	64.55
SU75_2	75	8	(0,2,2)	201.09	32.91	19.86	11000.00	324.00	11343.90	64.72
SU75_3	75	8	(0,2,2)	169.80	26.54	16.02	11000.00	229.00	11245.00	63.34
SU75_4	75	8	(0,2,2)	201.77	33.19	20.03	11000.00	240.00	11260.00	65.21
SU75_5	75	8	(0,2,2)	209.93	35.85	21.64	12500.00	331.00	12852.60	63.64
R75_1	75	8	(0,2,2)	172.62	29.32	17.70	11000.00	289.00	11306.70	63.91
R75_2	75	8	(0,2,2)	212.28	33.72	20.35	11000.00	278.00	11298.30	64.69
R75_3	75	8	(0,2,2)	207.77	61.32	37.00	11000.00	324.00	11361.00	63.58
R75_4	75	8	(0,2,2)	191.46	34.50	20.82	11000.00	289.00	11309.80	64.13
R75_5	75	8	(0,3,1)	205.30	32.22	19.44	11000.00	320.00	11339.40	63.80

Table A.4
Computational results on the 100-customer instances.

Instance	$\|\mathcal{N}_c\|$	$\|\mathcal{N}_0\|$	P-L-HALNS							
			Opened depots	Total distance (km)	CO_2 emissions (kg)	Fuel and CO_2 emissions costs (£)	Depot cost (£)	Vehicle cost (£)	Total cost (£)	Time (s)
CC100_1	100	10	(3,1,2)	145.59	34.20	20.64	22500.00	349.00	22869.60	159.53
CC100_2	100	10	(2,1,2)	125.57	36.64	22.11	17500.00	342.00	17864.10	176.07
CC100_3	100	10	(3,2,0)	143.70	70.06	42.27	22000.00	391.00	22433.30	176.89
CC100_4	100	10	(3,1,2)	143.15	38.26	23.09	22500.00	360.00	22883.10	178.28
CC100_5	100	10	(2,2,1)	143.21	38.88	23.46	19000.00	349.00	19372.50	156.76
SU100_1	100	10	(0,3,3)	236.50	41.44	25.01	14500.00	384.00	14909.00	167.88
SU100_2	100	10	(0,2,3)	242.52	43.71	26.38	14500.00	426.00	14952.40	146.06
SU100_3	100	10	(0,2,3)	246.52	38.64	23.32	14500.00	433.00	14956.30	147.51
SU100_4	100	10	(0,2,3)	255.20	44.68	26.96	16500.00	360.00	16887.00	147.15
SU100_5	100	10	(0,2,3)	241.49	41.61	25.11	14500.00	384.00	14909.10	147.17
R100_1	100	10	(0,3,2)	250.47	106.86	64.48	14500.00	380.00	14944.50	148.83
R100_2	100	10	(0,3,2)	262.33	43.66	26.35	13000.00	384.00	13410.30	147.92
R100_3	100	10	(0,3,2)	263.72	43.55	26.28	13000.00	398.00	13424.30	159.90
R100_4	100	10	(0,3,3)	257.90	42.53	25.67	13000.00	384.00	13409.70	157.72
R100_5	100	10	(0,3,2)	262.70	36.68	22.13	14500.00	433.00	14955.10	176.27

References

Albareda-Sambola, M., Díaz, J.A., Fernández, E., 2005. A compact model and tight bounds for a combined location-routing problem. Computers & Operations Research 32, 407–428.
Albareda-Sambola, M., 2015. Location-routing and location-arc routing problems. In: Laporte, G., Nickel, S., Saldanha da Gama, F. (Eds.), Location Science. Springer, Berlin-Heidelberg, pp. 399–418.
Baldacci, R., Battarra, M., Vigo, D., 2008. Routing a heterogeneous fleet of vehicles. In: Golden, B.L., Raghavan, S., Wasil, E.A. (Eds.), The Vehicle Routing Problem: Latest Advances and New Challenges. Springer, New York, pp. 1–25.
Barreto, S., 2004. Análise e modelização de problemas de localização-distribuição (Analysis and Modelling of Location-routing Problems). (Ph.d. thesis). University of Aveiro, Aveiro, Portugal.
Barth, M., Boriboonsomsin, K., 2008. Real-world CO_2 impacts of traffic congestion. Transportation Research Record: Journal of the Transportation Research Board 2058, 163–171.
Barth, M., Boriboonsomsin, K., 2009. Energy and emissions impacts of a freeway-based dynamic eco-driving system. Transportation Research Part D 14, 400–410.
Barth, M., Younglove, T., Scora, G., 2005. Development of a Heavy-duty Diesel Modal Emissions and Fuel Consumption Model. Technical report UCB-ITS-PRR-2005-1. California PATH Program. Institute of transportation Studies, University of California at Berkeley.
Bektaş, T., Laporte, G., 2011. The pollution-routing problem. Transportation Research Part B 45, 1232–1250.
Bigazzi, A.Y., Figliozzi, M.A., 2012. Congestion and emissions mitigation: a comparison of capacity, demand, and vehicle based strategies. Transportation Research Part D 17, 538–547.
Boudoin, D., Morel, C., Gardat, M., 2014. Supply chains and urban logistics platforms. In: Gonzalez-Feliu, J., Semet, F., Routhier, J.-L. (Eds.), Sustainable Urban Logistics: Concepts, Methods and Information Systems. Springer, Berlin-Heidelberg, pp. 1–20.
Clarke, G., Wright, J.W., 1964. Scheduling of vehicles from a central depot to a number of delivery points. Operations Research 12, 568–581.
Coe, E., 2005. Average Carbon Dioxide Emissions Resulting From Gasoline and Diesel Fuel. Technical report. United States Environmental Protection Agency. < http://www.epa.gov/otaq/climate/420f05001.pdf> (accessed 11.01.15)
Dablanc, L., 2014. Logistics sprawl and urban freight planning issues in a major gateway city. In: Gonzalez-Feliu, J., Semet, F., Routhier, J.-L. (Eds.), Sustainable Urban Logistics: Concepts, Methods and Information Systems. Springer, Berlin-Heidelberg, pp. 49–69.
Demir, E., Bektaş, T., Laporte, G., 2011. A comparative analysis of several vehicle emission models for road freight transportation. Transportation Research Part D 6, 347–357.
Demir, E., Bektaş, T., Laporte, G., 2012. An adaptive large neighborhood search heuristic for the pollution-routing problem. European Journal of Operational Research 223, 346–359.
Demir, E., Bektaş, T., Laporte, G., 2014a. The bi-objective pollution-routing problem. European Journal of Operational Research 232, 464–478.
Demir, E., Bektaş, T., Laporte, G., 2014b. A review of recent research on green road freight transportation. European Journal of Operational Research 237, 775–793.
DfT, 2012. Reducing Greenhouse Gases and Other Emissions From Transport. United Kingdom Department for Transport.< http://www.gov.uk/government/policies/reducing-greenhouse-gases-and-other-emissions-from-transport> (accessed 15.11.14)
DfT, 2013. Setting Local Speed Limits. United Kingdom Department for Transport.< https://www.gov.uk/government/uploads/system/uploads/attachment_data/file/63975/circular-01-2013.pdf> (accessed 10.12.14)
Drexl, M., Schneider, M., 2015. A survey of variants and extensions of the location-routing problem. European Journal of Operational Research 241, 283–308.
Dublin City Council, 2015. Speed Limits in Your Area. Dublin City Council.< http://www.dublincity.ie/main-menu-services-roads-and-traffic-general-traffic-measures/speed-limits-your-area> (accessed 10.11.15)
Eglese, R., Bektaş, T., 2014. Green vehicle routing. In: Toth, P., Vigo, D. (Eds.), Vehicle Routing: Problems, Methods, and Applications. MOS-SIAM Series on Optimization. Society for Industrial and Applied Mathematics, Philadelphia, pp. 437–458.
Ehmke, J.F., Campbell, A.M., Thomas, B.W., 2014. Solution Approaches for Stochastic Emissions-minimized Paths in Urban Areas. Technical report. University of Iowa, Iowa City.
EPA, 2012. DRAFT Inventory of United States Greenhouse Gas Emissions and Sinks: 1990–2012. United States Environmental Protection Agency, USA.< http://www.epa.gov/climatechange/Downloads/ghgemissions/US-GHG-Inventory-2014-Main-Text.pdf> (accessed 18.11.14)
Fatnassi, E., Chaouachi, J., Klibi, W., 2015. Planning and operating a shared goods and passengers on-demand rapid transit system for sustainable city-logistics. Transportation Research Part B 81, 440–460.
FHWA, 2011. Vehicle Types. United States Department of Transport, Federal Highway Administration, USA.< http://www.fhwa.dot.gov/policy/ohpi/vehclass.htm> (accessed 25.12.14)
Figliozzi, M.A., 2011. The impact of congestion on time-definitive urban freight distribution networks CO2 emission levels: results from a case study in Portland, Oregon. Transportation Research Part C 19, 766–778.
Franceschetti, A., Honhon, D., Van Woensel, T., Bektaş, T., Laporte, G., 2013. The time-dependent pollution-routing problem. Transportation Research Part B 56, 265–293.
Ghiani, G., Laporte, G., Musmanno, R., 2013. Introduction to Logistics Systems Management. Wiley, Chichester.
Golden, B.L., Assad, A.A., Levy, L., Gheysens, F., 1984. The fleet size and mix vehicle routing problem.. Computers & Operations Research 11, 49–66.
Gonzalez-Feliu, J., Semet, F., Routhier, J.-L., 2014. Sustainable Urban Logistics: Concepts, Methods and Information Systems. Springer, Berlin-Heidelberg.
Google Maps, 2015. <https://maps.google.com> (accessed 15.01.15).
Hoff, A., Andersson, H., Christiansen, M., Hasle, G., Løkketangen, A., 2010. Industrial aspects and literature survey: fleet composition and routing. Computers & Operations Research 37, 2041–2061.
Hvattum, L.M., Norstad, I., Fagerholt, K., Laporte, G., 2013. Analysis of an exact algorithm for the vessel speed optimization problem. Networks 62, 132–135.
Jabali, O., Gendreau, M., Laporte, G., 2012a. A continuous approximation model for the fleet composition problem. Transportation Research Part B 46, 1591–1606.
Jabali, O., Van Woensel, T., de Kok, A.G., 2012b. Analysis of travel times and CO_2 emissions in time-dependent vehicle routing. Production and Operations Management 21, 1060–1074.
Kirby, H.R., Hutton, B., McQuaid, R.W., Raeside, R., Zhang, X., 2000. Modelling the effects of transport policy levers on fuel efficiency and national fuel consumption. Transportation Research Part D 5, 265–282.
Kirkby, T., 2002. Memorandum by Kingston upon Hull City Council (RTS 152) – 20 mph Zones in Kingston Upon Hull. Select Committee on Transport, Local Government and the Regions.< http://www.publications.parliament.uk/pa/cm200102/cmselect/cmtlgr/557/557ap80.htm> (accessed 09.12.14)
Koç, Ç., Bektaş, T., Jabali, O., Laporte, G., 2014. The fleet size and mix pollution-routing problem. Transportation Research Part B 70, 239–254.
Koç, Ç., Bektaş, T., Jabali, O., Laporte, G., 2015a. A hybrid evolutionary algorithm for heterogeneous fleet vehicle routing problems. Computers & Operations Research 64, 11–27.
Koç, Ç., Bektaş, T., Jabali, O., Laporte, G., 2016a. The fleet size and mix location-routing problem with time windows: formulations and a heuristic algorithm. European Journal of Operational Research 248, 33–51.
Koç, Ç., Bektaş, T., Jabali, O., Laporte, G., 2016b. Thirty years of heterogeneous vehicle routing. European Journal of Operational Research 249, 1–21.
Kopfer, H.W., Kopfer, H., 2013. Emissions minimization vehicle routing problem in dependence of different vehicle classes. In: Kreowski, H.-J., Reiter, B.S., Thoben, K.-D. (Eds.), Dynamics in Logistics, Lecture Notes in Logistics. Springer, Berlin, pp. 49–58.
Kopfer, H.W., Schönberger, J., Kopfer, H., 2014. Reducing greenhouse gas emissions of a heterogeneous vehicle fleet. Flexible Services and Manufacturing Journal 26, 221–248.

Kramer, R., Subramanian, A., Vidal, T., Lucídio dos Anjos, F.C., 2015. A matheuristic approach for the pollution-routing problem. European Journal of Operational Research 243, 523–539.
Krause, E.F., 2012. Taxicab Geometry: An Adventure in Non-Euclidean Geometry. Dover Publications, New York.
Kwon, Y.J., Choi, Y.J., Lee, D.H., 2013. Heterogeneous fixed fleet vehicle routing considering carbon emission. Transportation Research Part D 23, 81–89.
Laporte, G., 1988. Location-routing problems. In: Golden, B.L., Assad, A.A. (Eds.), Vehicle Routing: Methods and Studies. North-Holland, Amsterdam, pp. 163–198.
Laporte, G., Ropke, S., Vidal, T., 2014. Heuristics for the vehicle routing problem. In: Toth, P., Vigo, D. (Eds.), Vehicle Routing: Problems, Methods and Applications. MOS-SIAM Series in Optimization. Society for Industrial and Applied Mathematics, Philadelphia, pp. 87–116.
Lin, C., Choy, K.L., Ho, G.T.S., Chung, S.H., Lam, H.Y., 2014. Survey of green vehicle routing problem: past and future trends. Expert Systems with Applications 41, 1118–1138.
Maden, W., Eglese, R., Black, D., 2010. Vehicle routing and scheduling with time-varying data: a case study. Journal of the Operational Research Society 61, 515–522.
MAN, 2015a. Trucks in distribution transport. <http://www.mantruckandbus.co.uk/en/trucks/start_trucks.html> (accessed 19.01.15).
MAN Engines, 2015b. <http://www.engines.man.eu/global/en/index.html#7906576> (accessed 19.01.15).
MAN Spec Sheets, 2015c. <http://www.man-bodybuilder.co.uk/specs/euro6/> (accessed 19.01.15).
Mancini, S., Gonzalez-Feliu, J., Crainic, T.G., 2014. Planning and optimization methods for advanced urban logistics systems at tactical level. In: Gonzalez-Feliu, J., Semet, F., Routhier, J.-L. (Eds.), Sustainable Urban Logistics: Concepts, Methods and Information Systems. Springer, Berlin-Heidelberg, pp. 145–164.
Min, H., Jayaraman, V., Srivastava, R., 1998. Combined location-routing problems: a synthesis and future research directions. European Journal of Operational Research 108, 1–15.
Nagy, G., Salhi, S., 2007. Location-routing: issues, models and methods. European Journal of Operational Research 177, 649–672.
Norstad, I., Fagerholt, K., Laporte, G., 2010. Tramp ship routing and scheduling with speed optimization. Transportation Research Part C 19, 853–865.
Oregon Department of Transportation, 2015. Setting speeds. <http://www.oregon.gov/ODOT/HWY/TRAFFIC-ROADWAY/docs/pdf/speed_final.pdf> (accessed 23.01.15).
Ottawa Transportation Committee, 2009. Speed zoning policy. <http://ottawa.ca/calendar/ottawa/citycouncil/trc/2009/10-07/ACS2009-COS-PWS-0021.htm> (accessed 25.01.15).
Pisinger, D., Ropke, S., 2007. A general heuristic for vehicle routing problems. Computers & Operations Research 34, 2403–2435.
Prodhon, C., 2006. Le problème de localisation-routage (The Location-routing Problem). (Ph.d. thesis). Troyes University of Technology, Troyes, France.
Prodhon, C., Prins, C., 2014. A survey of recent research on location-routing problems. European Journal of Operational Research 238, 1–17.
Ropke, S., Pisinger, D., 2006a. An adaptive large neighborhood search heuristic for the pickup and delivery problem with time windows. Transportation Science 40, 455–472.
Ropke, S., Pisinger, D., 2006b. A unified heuristic for a large class of vehicle routing problems with backhauls. European Journal of Operational Research 171, 750–775.
Scora, M., Barth, G., 2006. Comprehensive Modal Emission Model (CMEM), Version 3.01, Users Guide. Technical report, University of California, Riverside. <http://www.cert.ucr.edu/cmem/docs/CMEM_User_Guide_v3.01d.pdf> (accessed 25.11.14).
Speh, T.W., 2009. Understanding warehouse costs and risks. Warehousing Forum 24, 1–6.
Statista, 2013. Market share of truck manufacturers in Europe. <http://www.statista.com/statistics/265008/market-share-of-truck-manufacturers-in-europe/> (accessed 29.12.14).
Taillard, E., 1999. A heuristic column generation method for the heterogeneous fleet vehicle routing problem. RAIRO (Recherche Opérationnelle/Operations Research) 33, 1–14.
Taniguchi, E., Thompson, R.G., Yamada, T., van Duin, J.H.R., 2001. City Logistics: Network Modelling and Intelligent Transport Systems. Pergamon, Amsterdam.
UK Government, 2014. Speed Limits. UK Government.< https://www.gov.uk/speed-limits> (accessed 03.12.14)
Van Woensel, T., Creten, R.C., Vandaele, N., 2001. Managing the environmental externalities of traffic logistics: the issue of emissions. Production and Operations Management 10, 207–223.
Von Boventer, E., 1961. The relationship between transportation costs and location rent in transportation problems. Journal of Regional Science 3, 27–40.
Wikipedia, 2015. Speed limits by country. <http://en.wikipedia.org/wiki/Speed_limits_by_country> (accessed 02.05.15).
Zhang, Z., Wei, L., Lim, A., 2015. An evolutionary local search for the capacitated vehicle routing problem minimizing fuel consumption under three-dimensional loading constraints. Transportation Research Part B 82, 20–35.